Effect of using Organosilane with Crumb Rubber Modified Hot Mix Asphalt Mixtures

By

Aswin Kumar Srinivasan

A Thesis Presented in Partial Fulfilment
of the Requirements for the Degree
Master of Science

Approved November 2018 by the
Graduate Supervisory Committee

Kamil E. Kaloush, Chair
Michael Mamlouk
Jose Medina Campillo

ARIZONA STATE UNIVERSITY

December 2018

ABSTRACT

Crumb rubber use in asphalt mixtures by means of wet process technology has been in place for several years in the United States with good performance record; however, it has some shortcomings such as maintaining high mixing and compaction temperatures in the field production. Organosilane (OS), a nanotechnology chemical substantially improves the bonding between aggregate and asphalt by modifying the aggregate structure from hydrophilic to hydrophobic contributing to increased moisture resistance of conventional asphalt mixtures. Use of Organosilane also reduces the mixing and compaction temperatures and facilitates similar compaction effort at lower temperatures. The objective of this research study was first to perform a Superpave mix design for Crumb Rubber Modified Binder (CRMB) gap-graded mixture with and without Organosilane; and secondly, analyse the performance of CRMB mixtures with and without Organosilane by conducting various laboratory tests. Performance Grade (PG) 64-22 binder was used to create the gap-graded Hot Mix Asphalt (HMA) mixtures for this study. Laboratory tests included rotational viscometer binder test and mixtures tests: dynamic modulus, flow number, tensile strength ratio, and C* fracture test. Results from the tests indicated that the addition of Organosilane facilitated easier compaction efforts despite reduced mixing and compaction temperatures. Organosilane also modestly increased the moisture susceptibility and resistance to crack propagation yet retaining equal rutting resistance of the CRMB mixtures.

DEDICATION

This work is dedicated to my father Mr. Srinivasan, my mother Ms. Jayanthi and my brother Dr. Bharath Kumar. It would have not been possible without the support of them.

Thank you!

.

ACKNOWLEDGMENTS

I would like to express my sincere gratitude to my advisor Dr. Kamil Kaloush for giving me the opportunity to work with him, for the continuous support of my graduate study and related research, for his patience, motivation, and immense knowledge. I could not have imagined having a better advisor and mentor for my academic research.

I am extremely thankful to Dr. Michael Mamlouk and Dr. Jose Medina for serving on my committee and for providing valuable feedback on my research work.

I would like to extend my regards to Janak Shah, for supporting me throughout my thesis. Special thanks to Ramadan Salim and Dr. Akshay Gundla for providing expert knowledge, teaching me how to operate the equipment, perform mixture testing and for being available every time that I had a obstacle.

I would like to thank Zydex industries, Vadodara, India, for providing the Organosilane product.

I am grateful to Mr. Robert McGennis from HollyFrontier Corporation for providing information on Crumb Rubber practices being utilized by agencies and related documents and Mr. Thomas Ludlum for constantly providing the asphalt binder needed for this study. Finally, I would like to thank the company Crumb Rubber Manufacturers, Mesa for providing the Crumb Rubber and Southwest Asphalt, El Mirage pit for providing the aggregate.

TABLE OF CONTENTS

Page

CHAPTER Page

CHAPTER Page

CHAPTER Page

CHAPTER Page

LIST OF FIGURES

Figure Page

Figure Page

Figure Page

LIST OF TABLES

Table Page

LIST OF ACRONYMS

AASHTO	- American Association of State Highway Transportation Officials
AC	- Asphalt Content
AMPT	- Asphalt Mixture Performance Tester
AR	- Asphalt Rubber
ASTM	- American Society for Testing and Materials
CFT	- C* Fracture Test
CR	- Crumb Rubber
CRM	- Crumb Rubber Modified
CRMB	- Crumb Rubber Modified Binder
EST	- E* Stiffness Ratio
FN	- Flow Number
GTR	- Ground Tire Rubber
HMA	- Hot Mix Asphalt
IDT	- Indirect Tension
LTTP	- Long Term Pavement Performance
LVDT	- Linear Variable Differential Transducer
NCHRP	- National Co-operative Highway Research Program
NMAS	- Nominal Maximum Aggregate Size
OBC	- Optimum Binder Content
OS	- Organosilane

PG	- Performance Grade
RAR	- Reacted and Activated Rubber
RPM	- Revolutions Per Minute
RTR	- Recycled Tire Rubber
SGC	- Superpave Gyratory Compactor
SHRP	- Strategic Highway Research Program
SMA	- Stone Mastic Asphalt
SSD	- Saturated Surface Dry
TSR	- Tensile Strength Ratio
VECD	- Visco-Elastic Continuum Damage
VFA	- Voids Filled with Asphalt
VG	- Viscosity Grade
VMA	- Voids in Mineral Aggregate
ZT	- Zycotherm

1. INTRODUCTION

1.1 Background

Over 1 billion of scrap tire in stockpiles were in the United States in the year 1990. The count of scrap tires dropped to near 110 million in the year 2010. This drastic reduction in 20 years was achieved due to extended use and application for scrap tires that include: the automotive industry, sports fields surfacing, molded products, playgrounds and animal bedding, civil engineering applications such as rubberized asphalt pavements (Rubber Manufacturers Association 2011). More than 12 million scrap tires are used for crumb rubber modified asphalts (Willis, et al. 2012).

The main purpose of using Asphalt Rubber (AR) in Hot Mix Asphalts (HMA) is that it improves the performance in comparison with the virgin bitumen/binder. Crumb Rubber Modified Binder (CRMB) perform exceptionally well in a range of climatic and traffic conditions. The rubber increases the overall elasticity of the binder by stiffening it in the operating temperature ranges; which reduces pavement temperature susceptibility and improves resistance to permanent deformation (rutting) and fatigue (Caltrans, 2003). Despite various advantages of CRMB, the burdensome wet process of producing the asphalt rubber binder, involving very high temperature (over 180℃) for mixing and compaction activities. The Crumb rubber modified HMA mixtures require high compaction efforts due to their nature of workability.

Over 90 percent of the highways and roads in the United States highways are constructed by using HMA (Copeland, 2011). One main problem faced by HMA pavements is the potential of moisture damage. Most of the observed distresses are caused or compounded due to moisture penetration (Ajay Ranka, 2014). The penetrated moisture causes loss of strength and durability of pavements. Moisture enters the pavement through air voids and weakens the asphalt-aggregate structure by reducing cohesive strength leading cohesive failure of pavement. The failure in bonding i.e. cohesive and adhesive failures in asphalt pavements occur due to pore pressure, displacement, detachment, and interfacial tension. Displacement occurs due to stripping of asphalt from the aggregate caused by irregular asphalt film coating, traffic and freeze-thaw cycles which results in additional pavement distresses of several types. (Zaniewski J, 2006).

The penetrated moisture interacts with the aggregate surface, causing a change in pH. This results in change of polar type groups absorbed, leading formation of negatively charged electrical double layers that attracts molecules of water causing removal of asphalt (Ajay Ranka, 2014) (Kiggundu, 1988). This leads to stripping of asphalt.

When the Nanoparticle Organosilane product is added to the HMA mixtures it reacts with inorganic aggregate and modifies their surface. This modification improves the aggregate - asphalt bonding and results in an increase to moisture resistance. Organosilane also performs as a warm mix additive; it reduces mixing temperatures up to 15℃ and compaction temperature up to 30℃. It is hypothesized that Organosilane, when added with CRMB, it can potentially reduce the burdensome mixing temperature and hence the CRMB mixtures can be mixed and placed at a lower temperature without losing workability.

1.2. Study Objective

The objective of this study is to evaluate the effect of using Organosilane in modified Crumb rubber HMA mixes and compare the performance with conventional CRMB mixes. Of interest, the study is also intending to evaluate any potential benefits of reduction in mixing temperatures of CRMB mixtures in presence of Organosilane.

1.3. Scope of Work

The scope of this study included laboratory fabrication of CRMB mixtures by modifying a selected virgin binder with 20% of crumb rubber by weight of the binder; this is the conventional crumb rubber modification used in Arizona. A PG 64-22 binder was used for preparing HMA gap-graded mixtures; the binder was supplied by HollyFrontier terminal located in Glendale, Arizona. The Organosilane was supplied by Zydex Industries and added to the binder at 0.15 % by weight of binder. Two CRMB mixtures were designed and prepared, out of which one mixture was modified with Organosilane additive.

The laboratory tests to evaluate performance included the following

- Dynamic Modulus Test (AASHTO-T342) for stiffness evaluation
- Flow Number Test (AASHTO-TP79-13) for rutting evaluation
- Tensile Strength Ratio (AASHTO-T-283) to evaluate moisture susceptibility
- C* Fracture Test to evaluate crack propagation

1.4. Testing Conditions and Number of Tests

Testing conditions and the number of replicates used for each test are shown in Table 1.

Table 1. Number of tests conducted for each mixture

Test	Temperature/Frequency/ Loading Rate/Strain Levels	Replicates	Total Tests
Dynamic Modulus	5 Temperatures x 6 Frequencies	3	15
Flow Number	1 Temperature x 1 Loading Rate	3	3
Tensile Strength Ratio	1 Temperature x 2 Subsets	3	6
C* Fracture Test	1 Temperature x 5 Loading Rates	2	10

1.5. Report Organization

This report is divided into 7 chapters. Chapter 1 provided insight on introduction, background and scope of work. Chapter 2 provides the literature review on crumb rubber technologies, Organosilane additives, the Superpave mix design, and the laboratory tests performed. Chapter 3 details the materials used in this research and method of specimen's fabrication. Chapter 4 includes the SuperPave Mix Design and gives the optimum binder content for both mixtures. Chapter 5 details the laboratory experiments and the conditions in which they were performed. Chapters 6 discusses the effects of Organosilane additives on the CRMB mixture. Finally, Chapter 7, presents the statistical analysis of the test results; whereas Chapter 8 provides the conclusion derived from the study and some insight on possible future work.

2. LITERATURE REVIEW

2.1. Crumb Rubber

Asphalt rubber is the product of mixing of crumb rubber from waste tires and asphalt binder. The use of crumb rubber was first brought in to use by Charles McDonald, a City of Phoenix engineer. In his research he found that a minimum of 15 % of crumb rubber by weight of binder is needed to achieve desired benefits. The result of McDonald work was a patented process commonly referred to as wet mix process. In this process the asphalt binder is heated to 177 °C and then the crumb rubber was added to it. The mixture is mixed for 45 minutes the least to allowing the binder to digest the crumb rubber. This digestion period is necessary for the rubber to form cross polymer chains with the asphalt binder. The use of this technology has led to increase in mechanical properties of pavements, resistance to rutting, noise reduction, energy consumption and CO_2 emissions leading to sustainable approach by use of waste tires. (Way 2012).

2.1.1. Crumb Rubber Grinding Processes

Scrap tires are grounded to crumbs by various grinding methods, each producing particles of different properties, size and characteristics. According to NCAT report 12-09, most commonly adopted methods include: cracker mill process, granulator process, micromill process and the cryogenic process. A brief description of the methods is shown in Table 2.

Table 2. Grinding Methods for Scrap Tires (NCAT Report 12-09)

Name	Method	Size (mm)	Other Characteristics
Cracker mill	Most commonly used method. Grinding is controlled by the spacing and speeds of the drums. The rubber particles are reduced by tearing as it moves through a rotating corrugated steel drum.	5-0.5	High surface area. Irregular shapes. Usually done at ambient temperatures.
Granulator	Uses revolving steel plates to shred the tire particles.	9.5-0.5	Cubical particles. Low surface area.
Micromill	Water is mixed with crumb rubber to form a slurry which is then forced through an abrasive disk.	0.5-0.075	Reduces particle size beyond that of a granulator or cracker mill.
Cryogenic	Liquid nitrogen is used to increase the brittleness of the crumb rubber. Once frozen it can be ground to desired size.	0.6-0.05	Hammer mills and turbo mills are used to make different particle size.

2.1.2. Crumb Rubber Modified Binder (CRMB)

Crumb rubber modified asphalt binder exhibited an increase in softening point with a proportional increase in crumb rubber content. (by (Albayati et al. 2011; Khadivar and Kavussi, 2013; Mansob et al. 2014). The penetration values and ductile nature decreased with an increase in crumb rubber content due to the stiffening property, the elastic recovery was found to be maximum for 15% and least for 5 % CRMB. The study carried out by Navarro et al. (2005) conveyed that the CRMB has an increase in flexibility of binder at low temperatures due to the reduction in elastic and viscous moduli, whereas at high temperatures a significant increase in both moduli is observed relating to a more elastic binder property.

2.2. Organosilane

Inorganic materials such as aggregates in HMA mixes react with Organosilane compounds with modify their surface (Ajay Ranka, 2014). Organosilane is the organo functional alkoxysilane. The alkoxy group is radical in the organic chain, which imparts required characteristics with polymers. This alkyl group may be Epoxy, Chloro, Mecapto, Amino etc. The hydrophobic nature is imparted by the presence of alkyl group. Agents called silylating agents are used for the reaction occurring between mineral and polymer to yield a composite which retains properties in presence of moisture/wet conditions. This property of Organosilane changes hydrophilic (water loving) aggregates to hydrophobic (water hating) i.e. oil loving surfaces.

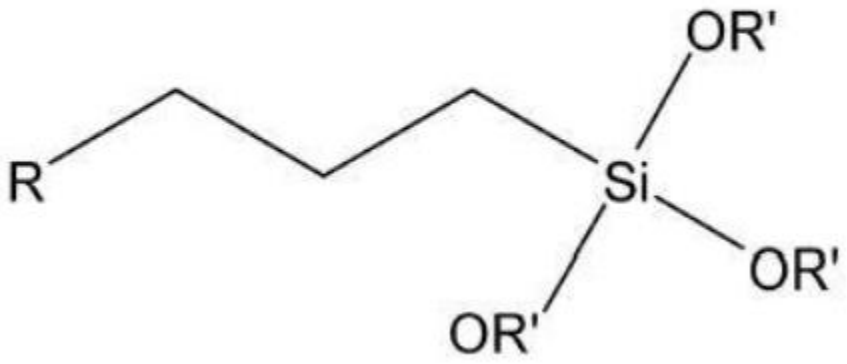

Figure 1. Organosilane alkylalkoxy compound. (Ajay Ranka, 2014)

The aggregate layer containing the hydroxy group form a silane bond with the alkoxy group present in the chain, this bond imparts the hydrophobic nature of the aggregate surface. The various possible reactions are shown in Figure 2. All the reactions are irreversible i.e. they stay hydrophobic due to the siloxane bond.

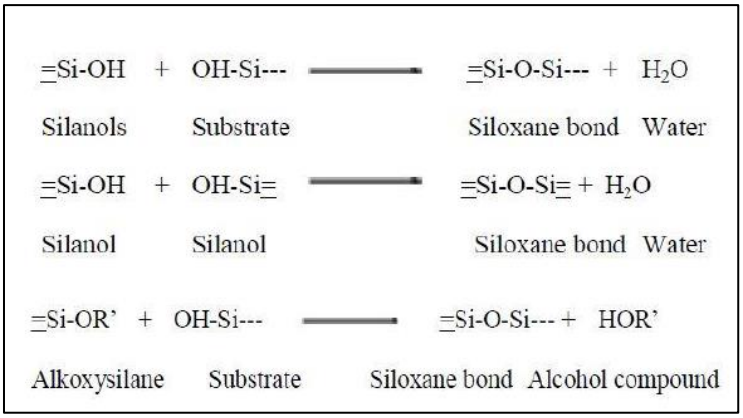

Figure 2. Substrate and organosilane – possible reactions (Ajay Ranka, 2014)

The reaction turns the surface of aggregate to oil loving, the oil in the mixture is asphalt, hence the aggregate has a better bonding with the non- polar asphalt in the mix. The reaction occurs at a Nano level region around the surface of the aggregate enabling bonding with asphalt. This interface at the surface of aggregates provides complete wetting of aggregates. This bond removes any air interface around the aggregate due to increased wetting, this air interphase responsible for intrusion of moisture causing stripping of asphalt is reduced. Figure 3 shows the microscopic reaction on the surface of the aggregate.

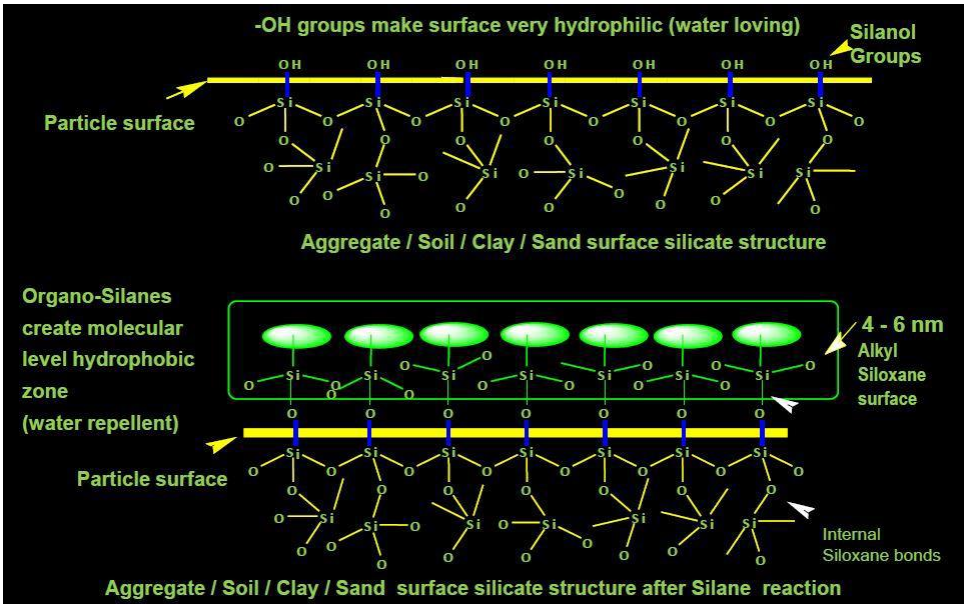

Figure 3. Reaction of silanes near the aggregate surface, (Ajay Ranka, 2014)

The Marshall stability increased under addition of Organosilane with 0.1% dosage at 115 °C in comparison with HMA mixes at 150°C. Also, the optimum binder content dropped by 0.05 % to 0.1 % for mixes with Organosilane. OBC should be found out individually for both HMA with and without Organosilane for varying temperatures and additive dosage rate. (Rohit N 2013).

Hasan and Hamzah (Hasan, et al. 2017) studies conveyed specimen prepared using Organosilane exhibit higher workability and easier compaction from the results of compaction data using the Servopac gyratory compactor, compared to the conventional mixture. From the mixture performance test results, mixtures prepared with Organosilane showed comparable if not better performance than the control sample in terms of the resistance to moisture damage, permanent deformation and cracking.

Raveesh and Manjunath (Raveesh J, 2017) evaluated the mechanical behavior of bitumen under the effect of ZT. The WMA produced by adding ZT to mix is compared to HMA. The study concluded that use of ZT in WMA reduced the mixing temperature and had given satisfactory results. The mix showed higher Marshall stability and moisture resistance than the HMA. WMA modified with ZT can become an alternative to HMA.

Mirzababaei (Mirzababaei, 2016) used dosages of ZT and by the results of Fourier Transformed Infrared spectroscopy (FTIR) reported that it creates a Si-O-Si hydrophobic layer over the surface enabling the wetting process. The study also conveys increase in Resilient Modulus Ratio, Fracture Energy Ratio and Tensile Strength Ratio.

2.2.1. Warm Mix Additives

The use of warm mix additives (WMA) in HMA for reduction in mixing and compaction temperatures have become a popular practice recently. Crumb rubber mixes require high compaction and mixing temperature for workability and desired compaction. Warm mix additives alter the viscosity or surface tension of the binder enabling better wetting at a lower temperature. The reduction in mixing temperature offered by warm mix additives also aid in less carbon foot print. There are several warm mix technologies that have been used in recent years but can be mainly classified in three groups: wax or organic additives, water foaming, and chemical additives (Table 3). Wax warm mix additives are generally prepared by coal gasification process and are generally referred to as Fischer-Tropsch (FT) paraffin wax which offers reduction by change is viscosity of binder. Sasobit is an example of a FT- Paraffin wax additive. Foaming warm mix additives consists a small amount of water added to hot asphalt. The water converts to steam, expands the binder and will be encapsulated in binder. The foamed binder improves aggregate wetting and reduces

viscosity of the binder. Zeolites can be used as an alternative to water in the hot binder. Zeolites are minerals that contain approximately 20% by weight of water, water is released, and the foamed asphalt is produced in hot environments.

Table 3. WMA Technology (After: Cheng, Lane and Hicks, 2012)

Product	Type of Additive
Rediset WMX	Chemical
CECABASE RT	Chemical
Aspha-min	Foaming
Double Barrel Green	Foaming
WAM Foam	Foaming
Green Machine	Foaming
Revix	Chemical
Hgrant Wamrm Mix System	Foaming
Evotherm	Chemical
Sasobit	Organic
Advera WMA	Foaming

Hydrated lime is very well used antistrip in HMA. It has the property to property to strip any moisture in the aggregates and offer better wetting of asphalt binder. Lime also offers other advantages such as acting as a mineral filler in the mix, increasing mechanical stiffness causing cause to increase in rut performance. Lime is a very good antistrip, but the difficulty in handling the dusty mass at workplace and control over the dosage posses a challenge. Warm mix additives offer the same benefits coupled with reduction is mixing and compaction temperatures. As the objective of this study is to evaluate the effect of Organosilane additives with CR HMA, offering reduction in temperatures and to evaluate the effect of this variation on performance properties.

The chemical warm mix additives alter the surface tension of the binder offering better wetting at lower temperatures. The additives modify the surface of the aggregate by replacing the hydroxyl groups making this hydrophobic. Most chemical additives have amines or silanes in their structures causing this mechanism. Divito et al. (1982) compared aggregates treated with silanes to aggregates treated with commercial amine anti-strip agents. Their results showed that silane treated aggregates have greater resistance to water damage than aggregates treated with commercial amine anti-strip agents. This supported the curiosity of evaluating the effect of Organosilane additive with CR HMA

2.3. SuperPave Mix Design

The Superpave mix design, SUPER performing PAVEment Mix design, procedure was developed as part of the first Strategic Highway Research Program (SHRP) in the early 1990s paving the way for contractors and engineers to design better pavements to sustain extreme temperatures and traffic. Superpave (as a whole) was shaped to make the best use of asphalt paving technology and to present a formula that would enhance asphalt mixtures resistance to deformation and cracking. The principal parts of the mix design are the Performance Grading (PG) system for asphalt binder and volumetric properties through compaction using the Superpave Gyratory compactors.

The main advantage of this mix design is the inclusion of materials properties and volumetric in to the selection criteria which affects the real time performance of the pavements. Superpave specifications generally require 94% compaction with an allowable variance of +/-2% of maximum theoretic value.

The contractors still can compact at higher levels in the field, but it is virtually impossible to achieve a density greater than 100%. If an HMA material was to be over compacted, this also result in a significantly reduced life. Volumetric properties must be met during production to ensure the projected long-term life of the pavement.

The existing Superpave system comprises of three interconnected elements: an asphalt binder specification, and a volumetric mix design and analysis system that is based on gyratory compaction. Performance-related models that take environmental factors into consideration. This last element has been erratic and inconsistent among several states sometimes states decide not to use any performance-related testing other than a moisture sensitivity test (AASHTO T 283); however, interest has grown in a switch from that test to the Hamburg Wheel Track Test (HWTT) for assessing both moisture sensitivity and rutting. Additionally, many states are using both AASHTO T 324 and T 283 or their own versions of those tests. One of the major changes made to the Superpave volumetric mix design procedure was most significantly the elimination of the "restricted zone" in aggregate gradations. Simplification of the N_{design} tables was another important change.

2.4. Asphalt Mixtures Laboratory Tests

2.4.1. Dynamic Modulus Test

The Dynamic Modulus (E*) laboratory test is one of the major input material properties for flexible pavement design. It has been recommended as a Simple Performance Test (SPT) under the National Cooperative Highway Research Program (NCHRP) Project.

The stress-to-strain relationship under a continuous sinusoidal loading for linear viscoelastic materials such as asphalt mixtures, the is defined by its complex dynamic modulus (E*). This is a complex number that relates stress to strain for linear viscoelastic materials subjected to continuously applied sinusoidal loading in the frequency domain. The ratio of the amplitude of the sinusoidal stress (at any given time, t, and angular load frequency, ω), $\dot{\sigma} = \sigma_0 \sin(\omega t)$ and the amplitude of the sinusoidal strain $\dot{\varepsilon} = \varepsilon_0 \sin(\omega t - \phi)$, at the same time and frequency, that results in a steady state response is defined as the complex modulus (Figure 4):

$$E^* = \frac{\sigma}{\varepsilon} = \frac{\sigma_0 e^{i\omega t}}{\varepsilon_0 e^{i(\omega t - \phi)}} = \frac{\sigma_0 \sin(\omega t)}{\varepsilon_0 \sin(\omega t - \phi)}$$

Where, σ_0 = peak (maximum) stress

ε_0 = Maximum strain

φ = phase angle in degrees

ω = angular velocity

t = time in seconds

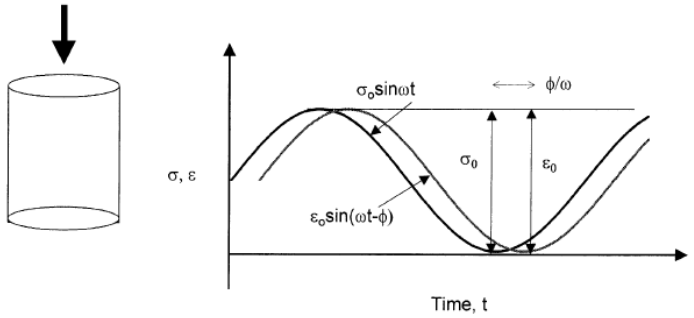

Figure 4. Stress pulse for the dynamic modulus test

The modulus of the asphalt mixture at all temperatures and time rate of load is determined from a master curve constructed at a reference temperature (generally taken as 21.1 °C). Master curves are constructed using the principle of time-temperature superposition. The data at various temperatures are shifted with respect to time until the curves merge into single smooth function. The time dependency of the material's Modulus value is given by the master curve, while the temperature dependency of the material is given by the amount of shifting at each temperature used to generate the master curve. In general, the master modulus curve can be mathematically modeled by a sigmoidal function described as:

$$\text{Log } |E^*| = \delta + \frac{\alpha}{1+e^{\beta+\gamma(\log t_r)}}$$

Where,

t_r = reduced time of loading at reference temperature

δ = minimum value of E*

$\delta+\alpha$ = maximum value of E*

β, γ = parameters describing the shape of the sigmoidal function

The shift factor can be shown in the following form:

$$a(T) = \frac{t}{t_r}$$

Where,

a(T) = shift factor as a function of temperature

t = time of loading at desired temperature

t_r = time of loading at reference temperature

T = temperature

A second order polynomial relationship between the logarithm of the shift factor i.e. log $a(T_i)$ and the temperature in degrees Fahrenheit (T_i) should be used.

The relationship can be expressed as follows:

$$\text{Log } a(T_i) = aT_i^2 + bT_i + c$$

Where,

$a(T_i)$ = shift factor as a function of temperature T_i

T = temperature of interest, °C

a, b and c = coefficients of the second order polynomial

2.4.2. Repeated Load Flow Number Test

The repeated dynamic load test for several thousand repetitions is employed as an approach to determine the permanent deformation characteristics of paving materials and the cumulative permanent deformation as a function of the number of cycles (repetitions) over the test period is recorded. Figure 5 illustrates the typical relationship between the total cumulative plastic strain and number of load cycles.

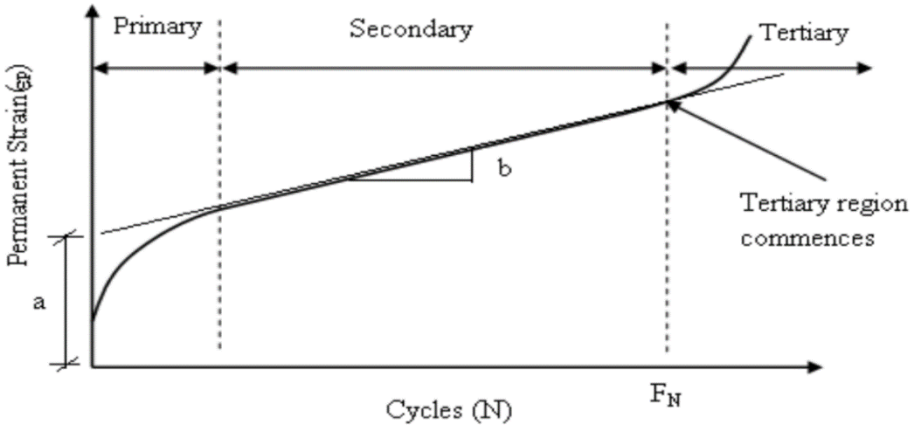

Figure 5. Permanent strain vs load cycle – Flow number test

The cumulative permanent strain curve is generally defined by three zones: primary, secondary, and tertiary. The primary zone is characterized by accumulation of permanent deformations rapidly. In secondary zone, the incremental permanent deformations decrease reaching a constant value. Finally, the incremental permanent deformations again increase, and permanent deformations accumulate rapidly in the tertiary zone. The flow cycle at which tertiary flow begins in the material is defined as flow number.

2.4.3. Tensile Strength Ratio

Moisture susceptibility is a prime factor in most of the pavement distresses. One of the prime issues of Crumb Rubber Modified mixes is their gradual loss of cohesion, which makes them very susceptible towards moisture resulting in shedding of aggregates and lesser durability (Moreno et al., 2010). Comparison of Tensile Strength Ratios is usually performed to evaluate moisture resistance, which includes taking the ratio of Indirect

tensile strengths, before and after conditioning immersed in water at high pavement temperature and follows the AASHTO T-283 testing protocol.

2.4.4. C* Fracture Test

The underlying principles of fracture mechanics govern the initiation and propagation of crack in materials. Sharp internal or surface notches which exist in numerous materials strengthen local stress distribution. When the stored energy in the material is equal or enough for new crack surface, the crack propagates. Material at the vicinity of the crack relaxes, the strain energy is consumed as surface energy, and the crack grows by an infinitesimal amount. If the rate of release of strain energy is equal to the fracture toughness, then the crack growth takes place under steady state conditions and the failure in unavoidable. The concept of fracture mechanics was first applied to asphalt concrete by Majidzadeh (1970). Abdulshafi (1992) had applied the energy (C*-Line Integral) approach to predicting the pavement fatigue life using the crack initiation, crack propagation, and failure. He concluded that two different tests are required to evaluate first the fatigue life to crack initiation (conventional fatigue testing) and second, the crack propagation phase using notched specimen testing under repeated loading. Abdulshafi and Majidzadeh used notched disk specimens to apply J-integral concept to the fracture and fatigue of asphalt pavements. Stempihar's (2013) dissertation work provided further development and refinement of the C* Fracture Test (CFT); Stempihar and Kaloush provided a summary of this work describing specimen geometry, test temperature variation, and a refined data analysis procedure.

The relation between the J-integral and the C* parameters is a method for measuring it experimentally. J is an energy rate and C* is an energy rate or power integral. An energy rate interpretation of J has been discussed by Landes and Begle (1976). J can be interpreted as the energy difference between the two identically loaded bodies having incrementally differing crack lengths.

$$J = -\frac{dU}{da}$$

Where,

U = Potential Energy

a = Crack Length

C* can be calculated in a similar manner using a power rate interpretation. Using this approach C* is the power difference between two identically loaded buddies having incrementally differing crack lengths.

$$C^* = -\frac{\partial U^*}{\partial a}$$

Where, U^* is the power or energy rate defined for a load p and displacement u by

$$U^* = \int_0^u p\,du$$

3. MATERIALS USED

3.1. Binder

A PG 64-22 binder was used to prepare the CRM mixtures with and without Organosilane. The binder was provided by HollyFrontier Refinery Terminal in Glendale, Arizona.

3.2. Aggregate

For this study, the aggregates were obtained from Southwest Asphalt El Mirage Pit and the materials used for composite gradation consisted of Blended sand, Crusher Fines, 3/8-inch aggregate and 3/4-inch aggregate.

Figure 6. Aggregate stockpiles in southwest asphalt el mirage pit

3.2.1. Aggregate Gradation for CRM Mix

A gap gradation with NMAS of 12.5mm (1/2-inch) was used to prepare the CRM mixtures. Aggregate gradation that contains only a small percentage of aggregate particles in the mid-size range is referred to as gap gradation. The mid-range of the curve is mostly flat. This gap facilitates space for rubber particles and additional binder to take position and create better bond. The aggregate stockpiles obtained from the pit were heated in an oven at 110°C overnight to remove all the moisture from it before sieving them into different sizes (AASHTO T 2). The Specification Bands were taken based on type of gradation and NMAS described under Superpave specifications from AASHTO MP 2. Figure 7 shows the gap gradation for the CRM mixture with Superpave control limits. The same gradation was used for the CRM mixtures with and without additive.

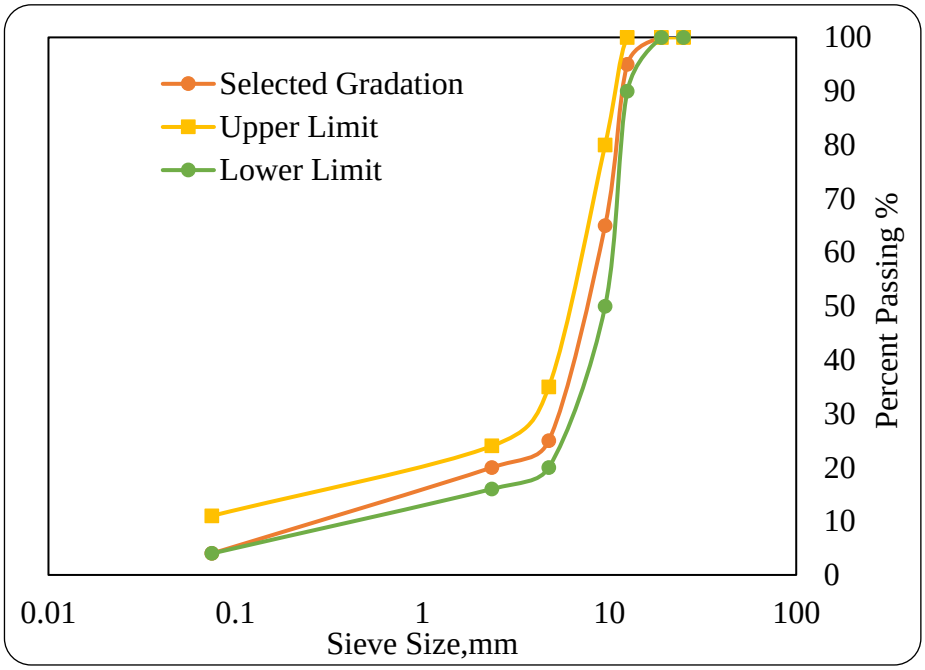

Figure 7. Gap gradation for both mixtures with specification bands

3.3. Crumb Rubber

The crumb rubber for this study was provided by Crumb Rubber Manufacturers, Mesa (Figure 8). A #30 mesh maximum particle size was selected being most commonly used.

Figure 8. Crumb Rubber (CR)

3.3.1. Crumb Rubber Modified Binder (CRMB) Preparation

CRMB was prepared by adding 20% crumb rubber (by weight of total binder) to the PG 64-22 Binder. The binder was heated to reach a temperature 177°C before setting it up in the mixing apparatus. The crumb rubber was added to the binder using a blender (low shear) at an rpm range of 800-1000 at temperature of 177℃ for 45 mins to let the crumb rubber swell (reaction). Figure 9 shows the mixer used for mixing crumb rubber with the binder.

Figure 9. Blender used for preparing crumb rubber modified binder

Figure 10 shows the CRMB after mixing. The effect of mixing Crumb Rubber can be easily seen from the gritty texture of the CRMB.

Figure 10 . CRMB

3.4. Organosilane / Zycotherm

Organosilane is the Organo functional alkoxysilane. In this study, Organosilane (OS) used was Zycotherm from Zydex Industries, Vadodara, India. It was prepared by using 3C nanotechnology by the manufacturer. OS is an anti-stripping additive and is generally stored at 5-45°C and making sure no moisture is in contact to maintain the effectiveness.

3.4.1. Dosage

The dosage of Organosilane depends upon the type of binder used. For CRMB, the recommended dosage as per manufacturer is 0.15 % by weight of virgin binder used in CRMB preparation.

3.4.2. Mixing Organosilane with CRMB

The quantity of OS to be mixed with the binder is relatively small. For an OS dosage of 0.15%, for 1000 grams of virgin binder, the amount of OS is 1.5 grams. The specific gravity of Organosilane is considered as 1, hence 1.5 grams equals 1.5 ml. A dry and disposable 1ml syringe with 0.1 ml scale was used to add drops of OS to the binder. The binder and OS were mixed at 177°C by using mechanical stirrer which can produce 20 to 30 mm deep vertex in asphalt (Figure 3-5). OS was added at 10 drops per minute in center of the vertex as shown in Figure 3.6 while stirrer speed is constant and should be left stirred for 5-10 minutes for complete mixing after adding OS. After Organosilane is mixed with binder, crumb rubber was added further, and the procedure was followed as previously stated for CRMB with Organosilane.

Figure 11. Zycotherm bottle and the syringe used for binder preparation

3.4.3. Rotaional Viscometer Binder Test

Preliminary viscosity tests were carried out as per AASHTO T 316 to see the effect of adding zyoctherm to CR; the original hypothesis was that Organosilane causes reduction in visocity leading to reduction in mixing temperature. However, the results showed no general reduction in visocity (Figures 12 and 13). Upon further investigation and per the literature review cited, Organosilane reduces the surface tension of the binder. This allows better wetting and efficient coating of aggregates, including fines. It also lends additional workability to the HMA, and mixing becomes easier (lower energy for mixing). Reduced surface tension leads to better wetting and efficient coating at lower temperatures, (typically lower by 15°C than normal mixing temperature). Upon further discussion with the manufacturere it was decided to reduce the mixing temperature of the CRMB by by 15°C. So, if the normal mixing temp for CRMB mixes is 175°C, it can be dropped down to 160°C with the use of Organosilane.

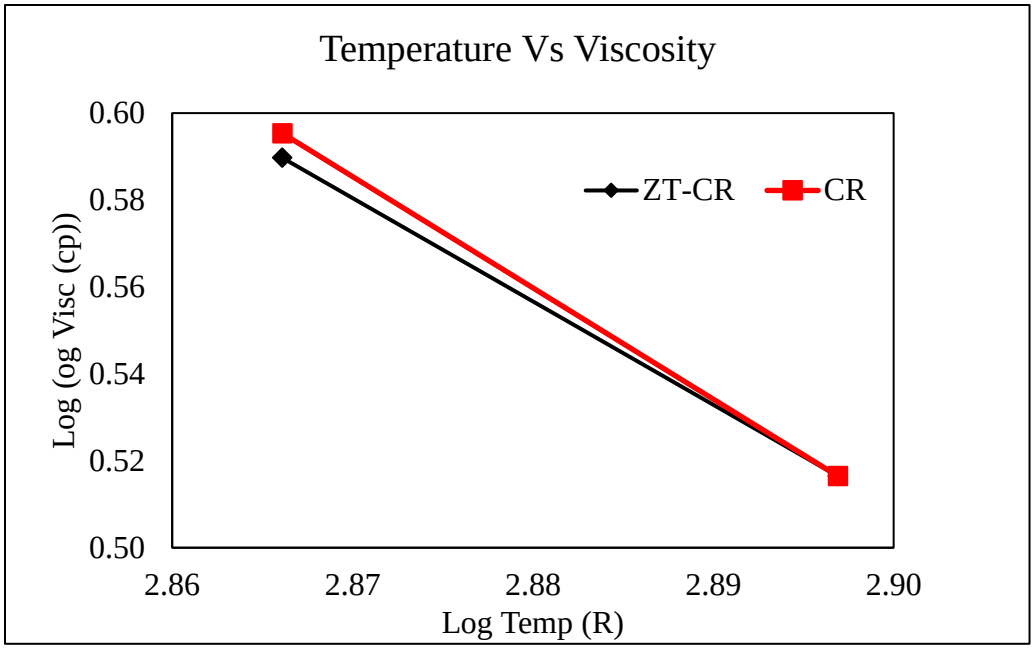

Figure 12. Viscosity vs. Temperature

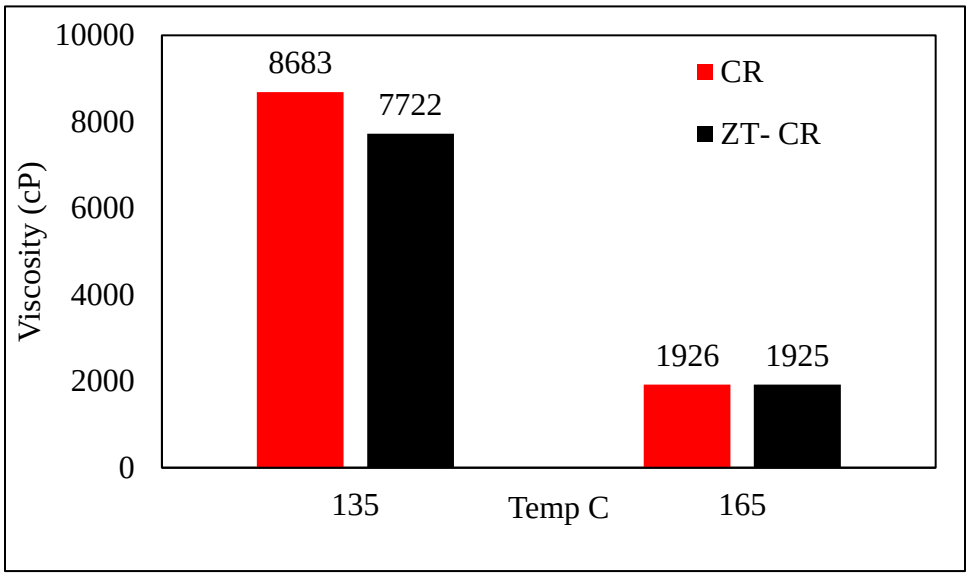

Figure 13. Viscosity comparison at different temperatures

3.5. Mixture Preparation

3.5.1. CRMB HMA

The Aggregates were heated to 175 °C overnight. The CRMB was heated at 175°C for 2 hours before mixing. The HMA mixture was then subjected to short-term aging of 4 hours at a temperature of 135°C. Then the mix was placed into molds and heated for 60 mins at 165°C before compaction. The compacted samples were released from mould after 30 mins.

3.5.2. CRMB with Organosilane

The Aggregates were heated to 160 °C overnight. The CRMB was heated at 160°C for 2 hours before mixing. This mixture has a lower mixing and compaction temperature than the conventional CRM mix due to presence of Organosilane additive, Organosilane. This mix was then subjected to short-term aging of 4 hours at a temperature of 135°C. Then the mix was placed into molds and heated for 60 mins at 160°C before compaction. The sample was released from mold after 30 mins.

4. SUPERPAVE MIX DESIGN

In general, pavement designs criteria address two major pavement distresses i. Rutting, occurring due to low shear resistance in material and flow, ii. Cracking which occurs when an asphalt layer tensile stress exceeds the tensile strength. The Superpave design system consists of three correlated components:

1) Binder specification of asphalt / binder

2) Volumetric analysis of mix design from compaction parameters.

3) Performance evaluation through laboratory testing.

Apart from the above parameters the Superpave also takes traffic load into consideration. The use of gyratory compactors for production of cylindrical test specimens is incorporated in the Superpave mix design. The compaction load is applied on the sample's top while the sample is inclined at 1.25 degrees. This compaction best represents the field compaction efforts.

The Superpave mix design procedure takes places in the following steps:

(1) PG Binder Selection

A PG binder grade is selected based upon the average seven-day maximum pavement temperature and the expected minimum pavement temperature. This entirely depends upon the region where the pavement is going to placed. A PG 64-22 was selected for preparation of CRM mixtures in this study.

(2) Aggregate Selection

Aggregate structure must meet the consensus properties such as angularity of coarse aggregates, percentage of flat and elongated particles, fine aggregate angularity, and clay content. Trials compactions are performed to evaluate dust proportion, volumetric and properties against the Superpave criteria. Trails are made to find out the optimum binder content for the composition in consideration.

(3) Sample preparation

A minimum of two specimens are prepared at each of the four binder contents (by total weight of mixture [TWM]): estimated binder content, estimated binder content ±0.5%, and estimated binder content +1.0%. These specimens are compacted to N_{max}.

(4) Analysis of Volumetric data

From the measured bulk specific gravity, compaction densities at different levels of gyration are back calculated. Volumetric properties (%VMA and %VFA) and dust proportion are calculated at N_{design}. The properties are plotted against their respective binder contents

(5) Selection of Optimal binder Content

The binder content corresponding to 4 % air voids is chosen as the Optimum Binder Content (OBC). Volumetric properties, dust proportion, and compaction density at $N_{initial}$ and $N_{maximum}$ are calculated and then verified at the OBC.

4.1. Crumb Rubber Mix

4.1.1 Sample Preparation

Three asphalt binder content 6.5%, 7.0% and 7.5% were selected with 20% Crumb rubber (by weight of total binder) for optimum asphalt binder percent selection using the Superpave mix design procedure. Two samples of 150 mm (6-inch) diameter cylinder approximately 115 mm (4.5 inches) in height and weight of 4700 grams were compacted (Figure 14) for every binder content respectively. Servopac Gyratory Compactor was used for compaction. A flat and circular load was applied with a diameter of 149.5 mm and a compaction pressure of 600 kPa (87 psi). For traffic level 3 to < 10 million Design ESALs, $N_{initial}$ = 8, N_{design} = 100, $N_{maximum}$ = 160. The mixture preparation procedure followed was same as described earlier. The short-term aging for mix design preparation was limited to 2 hours. The maximum specific gravity (AASHTO T 209) was determined for each percentage. The same procedure was followed with OS added Crum Rubber binder for Mix design.

Figure 14. Compacted superpave mix design samples

4.2. Optimum Binder Content and Volumetric Properties

An optimum binder content of 6.7 % was determined for the CRM mix. An optimum binder content of 6.75 % was determined for the CRM mix with Organosilane. The volumetric properties at optimum binder contents for each mixture are summarized in Table 4 below.

Table 4. Mixtures' volumetric properties

Property	CR	CR+ZT	Criteria
NMAS	1/2 inch	1/2 inch	-
OBC %	6.7 %	6.8 %	-
Va%	4 %	4 %	4%
VFA%	77 %	77.5 %	65 -75 %
VMA%	17.63 %	18 %	14 % min
DP	0.6	0.6	0.6-1.2

VFA represents the portion of the voids in the mineral aggregate that contain binder. The criteria for VFA depends on traffic level and the existing specifications doesn't take into consideration Crumb Rubber Modified Mixes. VFA is a somewhat redundant term since it is a function of air voids and VMA (Roberts et al., 1996). VFA is inversely related to air voids; as the air voids decreases, the VFA increases.

The gap graded mixes were compacted to 4% air voids and the mixes had high volume of effective binder which leads to increased VFA, if not, the interlock of aggregates would not have been good enough.

5. LABORATORY TESTS PERFORMED

5.1. Dynamic Modulus Test

5.1.1. Summary of Test Method

The AASHTO T 342 was followed for Dynamic Modulus - E* testing. Three replicates were used for each mix. E* tests were conducted at -10, 4.4, 21.1, 37.8 and 54.4 °C and 25, 10, 5, 1, 0.5 and 0.1 Hz loading frequencies. A rest period of 60 seconds was used between each frequency to allow some specimen recovery before the next loading

5.1.1 Test Specimen Preparation

A cut and cored cylindrical specimen of height 150 mm and diameter 100 mm is used for the Dynamic modulus test. The deformations in the axial directions were measured using three spring loaded Linear Variable Differential Transducers (LVDTs) placed vertically along the height of the cylindrical specimen. A pair of studs were glued to the cylindrical surface of the specimen for each LVDT, hence the three pair were glued such that the angle between any two given LVDT is 120° (Figure 41 Appendix C). The location of the studs is equal from the top and bottom of the specimen and are 100 mm apart. To eliminate any friction present between the loading plate and the specimen, two rubber membrane with vacuum grease between them were placed on top and bottom of the specimen (Figure 16). This warrants any friction present between plate and the surface of the specimen.

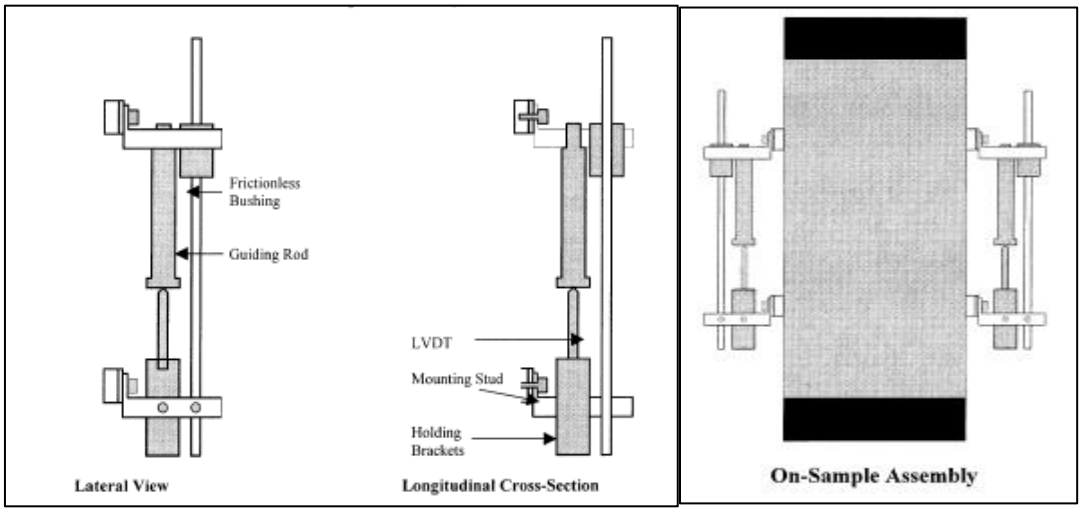

Figure 15. Axial LVDTs instrumentation

Figure 16. Instrumented dynamic modulus |E*| test sample

5.2. Repeated Load/ Flow Number Test

5.2.1 Summary of Test Method

Repeated load test was carried out on both the mixes, cylindrical specimens, 100 mm in diameter and 150 mm in height were used for the testing. The Flow Number (FN) is one of the performance tests relates to rutting resistance of asphalt mixtures. The FN is measured using repeated load testing. In this test, haversine axial compressive load pulses are applied to the specimen (Witczak M.W, 2002) (Bonaquist, 2012). The deformations are measured in a similar fashion and setup used in Chapter 5.1.1. Thin and fully lubricated membranes at the test specimen ends were used to warrant frictionless surface conditions (Figure 17). All tests were conducted within an environmentally controlled chamber throughout the testing. The tests were conducted unconfined at 50 °C and at a stress level of 400 kPa (58 psi). The test was conducted following (AASHTO-TP79-15, 2016).

Figure 17. Set-up specimen for flow number test

5.3. Tensile Strength Ratio

5.3.1. Conditioning of samples

A. One of the subsets were conditioned prior to testing indirect tensile strength.

B. The specimens were subjected to vacuum saturation with a minimum of 25mm water level above the specimens.

C. Saturation of the samples is achieved by subjecting the samples to a Vacuum of 13 to 67 kPa (10 to 26 in. Hg partial pressure) absolute pressure for 5 to 10 min.

D. The dry weight (A gm.) of the specimen and the surface saturated dry mass (B' gm) of the vacuum saturated was recorded and percentage saturation (S') was calculated as show in step E.

E. $S' = 100 * \frac{(B' - A)}{Va}$

F. where Volume of air voids $Va = Pa * \frac{E}{100}\ cm^3$

G. P_a is the percentage air voids in specimen and E is the volume of specimen in cm^3

H. A 70- 80 degree of saturation is preferred. Any sample with more saturation than 80 % is trashed.

I. The specimens were wrapped tightly using saran wrap (Figure 18) and were placed into the plastic bag with 10 ml of water in it and were sealed and cooled at -18°C for a minimum of 16 hours.

J. After the freeze cycle, the samples were placed in the hot water bath conditioned at 60 °C with at least an inch of water (25 mm) above the specimen surface for 24 hours and then removed.

5.3.2. Summary of Test Method

The indirect tensile strengths of moisture conditioned, and unconditioned asphalt samples are compared. The samples are conditions as stated in the previous section. The samples are brought to the room temperature by conditioning at 25°C for 2 hours after the freeze – thaw cycle. Both the conditioned and unconditioned specimens are diametrically loaded to test their Indirect Tensile Strength (Figure 48 Appendix C) . The calculations for Tensile Strength Ratio are calculated as follows:

$$\sigma = \frac{2S}{\pi * t * d}$$

Where σ is the strength of cylindrical sample, MPa

S is the maximum indirect tensile load sustained by the specimen, N

t is the thickness of cylindrical sample, mm

d is the diameter of cylindrical sample, mm

Tensile strength ratio is defined as ratio of Tensile strength of condoned samples to unconditioned samples and is given by,

$$TSR = \frac{\sigma_C}{\sigma_{UC}}$$

Where σ_C is the conditioned tensile strength of the asphalt mixture specimen and σ_{UC} is the unconditioned tensile strength of the asphalt mixture specimen

Figure 18. Dry and conditioned subsets for TSR

5.4. C* Fracture Test

5.4.1. Specimen Preparation

The circular disk specimens were produced by cutting two disks of 50 mm thick each from the center of a 150mm diameter by 180 mm tall gyratory compacted sample. A "V" shaped right-angle notch (25 mm deep) was carefully cut into the specimen. Using a saw blade, a slit of 3 mm deep by 1.6 mm wide was made for initial crack to propagate. The specimen is painted in white color and marked with lines with interval of 10 mm (Figure 20). A servo-hydraulic, Universal Testing Machine with 100kN load capacity and environmental control chamber was used to test the specimen. Crack propagation was recorded using a high-end video camera (Figure 31 Appendix C), the video was later used in analysis for crack propagation with respect to time elapsed.

5.4.2. Method for C* Determination

The method to determine C* star and crack growth rate a* is followed as per Stempihar, 2013.

- The data is collected as load versus displacement rate with respect to time for a given loading rate for specimens tested.
- For every displacement rate, the load value is adjusted by dividing it with sample thickness, then load and crack length as a function of time are plotted
- The load and the displacement rates are plotted for each crack length. The area under the curve in step above yields the energy rate input U* for the specimen. End area method is used to calculate the area under the curve. After that, the U* values were obtained and plotted versus crack length for each displacement rate. The slope of these curves is C* value for each displacement rate.
- At each displacement, the crack growth rate is calculated as total crack length divided by time elapsed. These values also were adjusted according to the specimen thickness. For all specimens, the crack growth rate a* versus the displacement were plotted
- Finally, the crack propagation rate (a*) was plotted with respect to C* for the specimens. The performance was evaluated using the slope of the resulting graph.

As per Stempihar's research (Stempihar 2013), A temperature of 10°C (50°F) is recommended for general comparison between mixtures. The following loading rates were used for both CR and ZT – CR mixes to evaluate their crack propagation properties at 10°C.

Table 5. Displacement rates used for the mixtures

Displacement Rate, Δ* (mm/min)	Displacement Rate, Δ* (mm/sec)
0.150	0.0025
0.228	0.0038
0.300	0.005
0.378	0.0063
0.450	0.0075

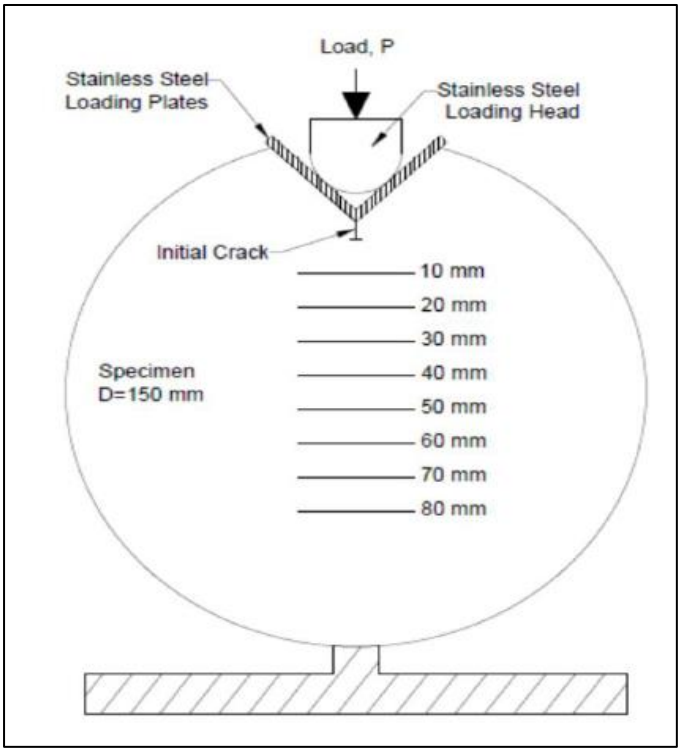

Figure 19. Schematic representation of C* Sample, Stempihar 2013

Figure 20. Actual C* sample prior to testing

6. RESULTS AND ANALYSIS

6.1. Dynamic Modulus Test

The E* values of the two mixes were compared for 6 frequencies and 5 temperatures. The Master Curve (Figure 21) below shows that ZT modified mix has slightly lower moduli at lower temperatures, a desirable property for better resistance to low temperature cracking. The ZT - CR mixes have higher modulus when compared to CR mix at higher temperatures; in general, and as temperature increases to the highest level, the modulus would be more a function of aggregates rather binder. Due to the formation of silane bond on the surface of the aggregate, the binder for the ZT-CR mix is wrapped around the aggregate surface more efficiently than the CR mix, contributing to slightly higher modulus at higher temperature. That is, the binder's property or role is better retained at higher temperatures in the case of ZT – CR mix.

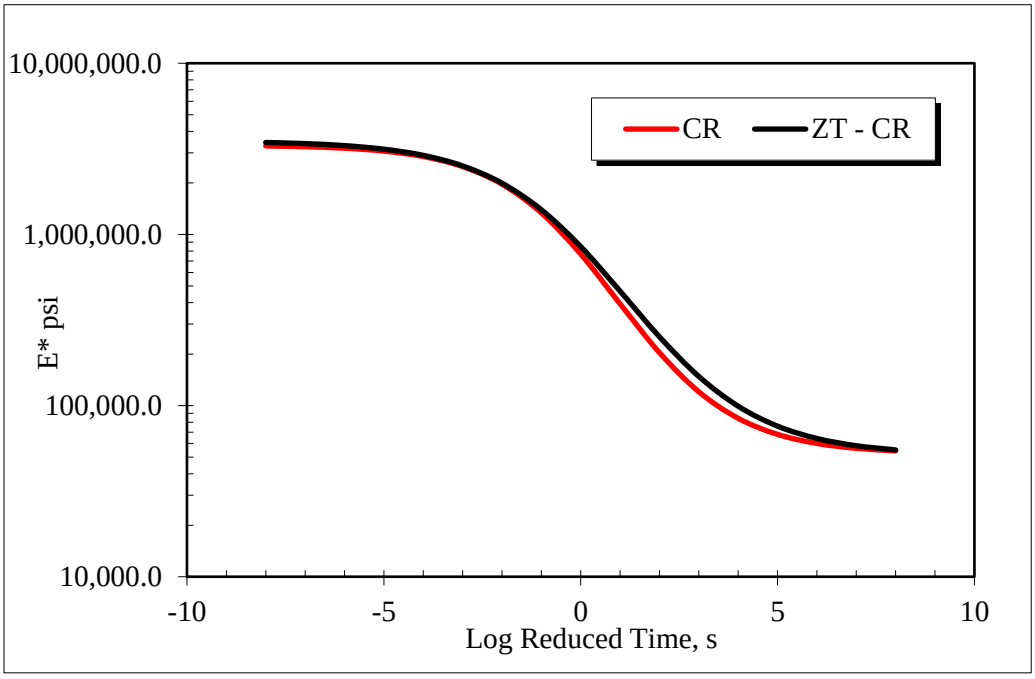

Figure 21. Master curve - average E* values of both mixtures

6.1.1. Comparison of Results by Frequency and Temperature

To better compare the results, the moduli from the dynamic modulus tests are compared for each mix at the specific combinations of frequencies and temperatures. The moduli values were plotted against frequency for each temperature. (Figures 22 - 26)

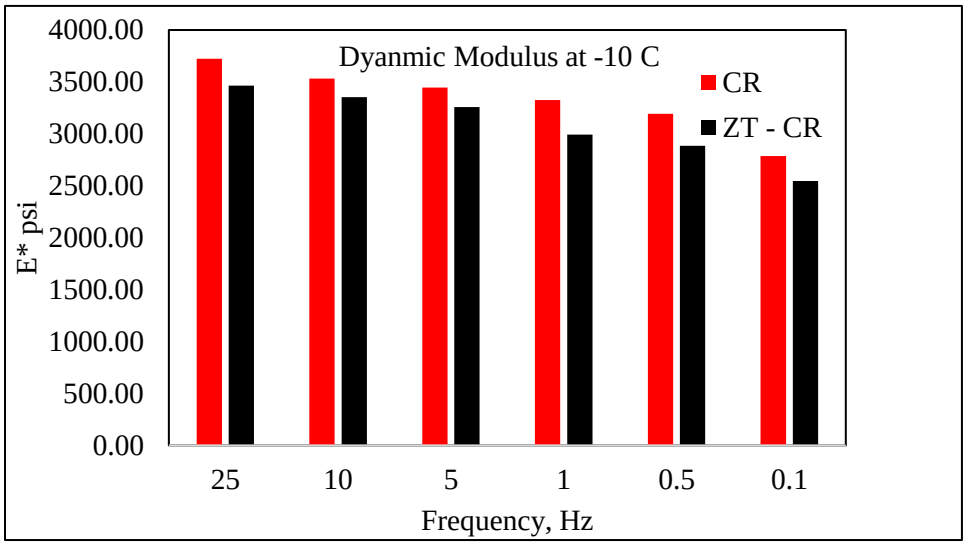

Figure 22. Modulus comparison at all frequencies for -10°C

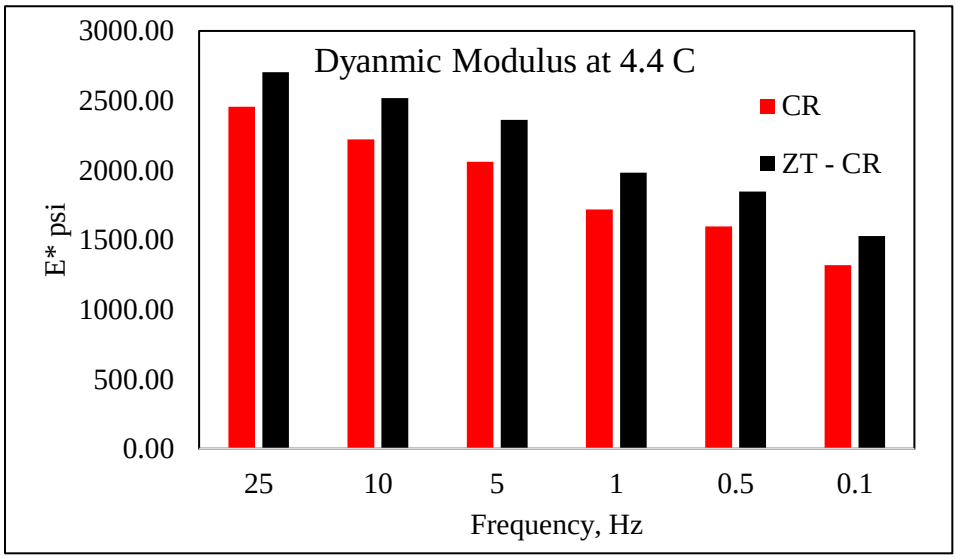

Figure 23. Modulus comparison at all frequencies for 4.4°C

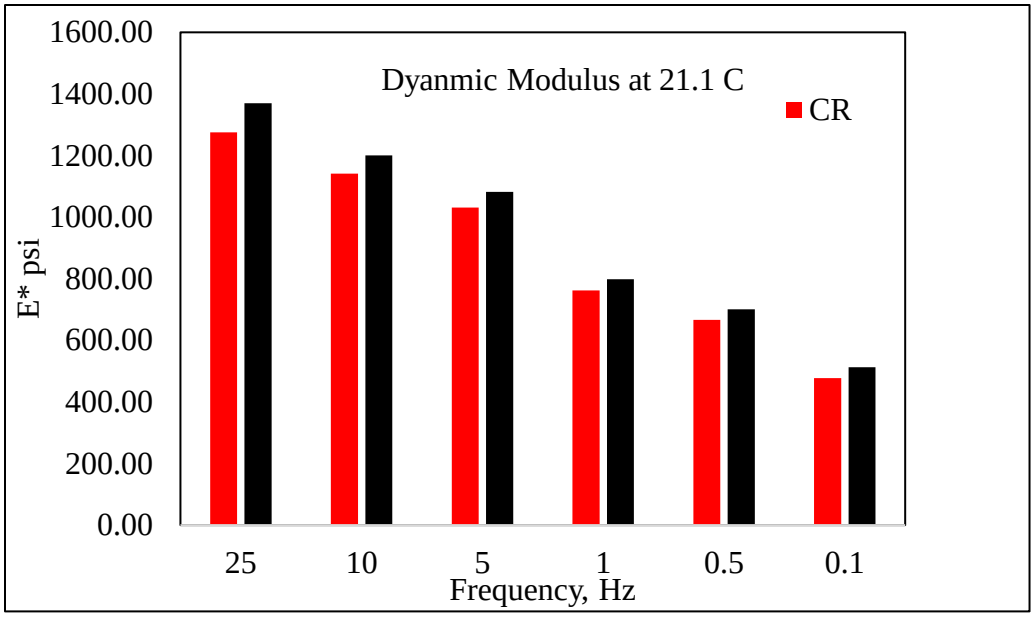

Figure 24. Modulus comparison at all frequencies for 21.1°C

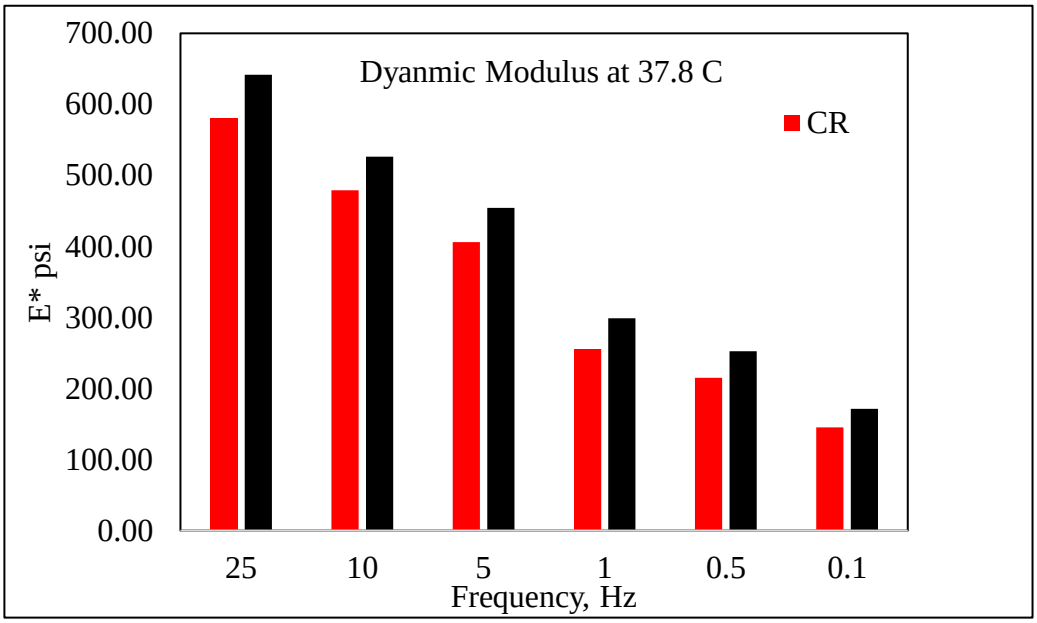

Figure 25. Modulus comparison at all frequencies for 37.8°C

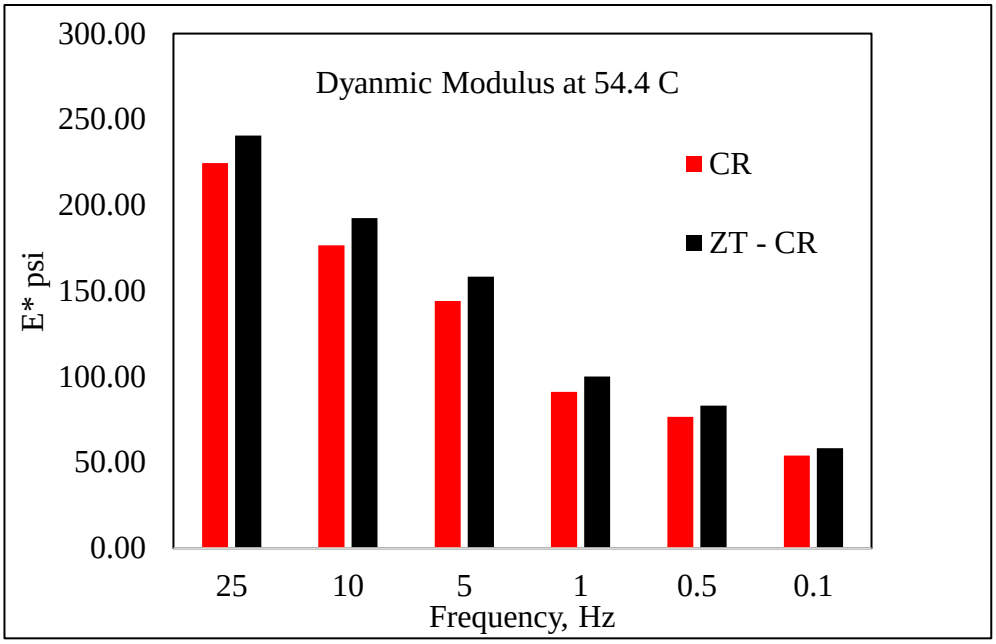

Figure 26. Modulus comparison at all frequencies for 54.4°C

6.2. Flow Number Test

Samples for both mixtures were tested at a deviator loading stress of 400KPa and a temperature of 50°C. The results for the Flow Number test are summarized in this section. On the average, the result showed the ZT – CR mixes had higher flow number value when compared to the CR mixes, but mostly they are close when the strain %, resilient modulus are taken into considerations. As explained earlier at higher temperatures, the better wetting of ZT – CR mixes due to the Organosilane bond possibly gave slightly a better resistance to flow as there is better bonding between aggregates due to increased asphalt binder wetting.

Table 6. Summary of flow number test results

Sample	CR			ZT - CR		
	Rep 1	Rep 2	Rep 2	Rep 1	Rep 2	Rep 3
Flow Number (Cycles)	1247	1479	1575	1911	1447	3095
Resilient Modulus at Failure (Mpa)	736.53	758.77	737.00	772.95	678.11	723.57
Axial Permanent Strain at Failure εp (%)	1.54	1.62	1.68	1.03	1.48	1.52
Axial Resilient Strain at Failure εr (%)	0.053	0.051	0.050	0.050	0.057	0.053
εp/εr (%)	29.11	31.73	33.56	20.58	25.91	28.60

The flow number results for both mixes are not statistically different, and this is verified in Chapter 7. The addition of Organosilane does not add any significant benefit to the flow property of the materials.

6.3. Tensile Strength Ratio (TSR)

The moisture resistance of mixes was evaluated using TSR. The test was conducted by following AASHTO T 283. The load rate of 50 mm/min was applied on the test samples. The results for the CR and ZT - CR are shown in Table 7-8. A minimum TSR of 0.70 (70%) to 0.80 (80%) is often preferred. But for gap graded mixtures, even a lower TSR value (65%) is considered acceptable. (Nadkarni et al, 2009). The complete TSR calculations are provided in Table 24 -25 in Appendix C

The ZT - CR mixes had more moisture resistance when compared to the CR mix, this was also explained with the enhanced coating of binder on the surface of the aggregate.

Table 7. TSR results for CR mix

CR Mix	**Conditioned**			**Dry (Unconditioned)**		
Average Air Voids	6.03%			6.06%		
Tensile strength (kPa)	645.7	741.7	629.3	1072	827.7	938.5
Average tensile strength (kPa)	672.2			946.1		
Tensile Strength Ratio (%)	71%					

Table 8. TSR results for ZT – CR mix

ZT - CR Mix	**Conditioned**			**Dry (Unconditioned)**		
Average Air Voids	6.06%			6.03%		
Tensile strength (kPa)	748.7	895.9	465.7	913.2	1028	711.8
Average tensile strength (kPa)	703.5			884.5		
Tensile Strength Ratio (%)	80%					

The lower cohesive strength in CR mix when compared to ZT - CR mixes explains the comparatively low moisture resistance and stripping of asphalt from aggregate is majorly caused due to the uneven coating of asphalt. Organosilane / Organosilane reacts with inorganic aggregate and modifies their surface. This modification improves the aggregates bonding with asphalt and increases the stripping resistance

6.4. C* Fracture Test

The Crack Growth Rate a* versus the C* (Figure 27) was plotted for both the mixes to compare the crack resistance offered at low temperatures. The slope of the graph represents the material's resistance to crack propagation, the higher the slope the less resistance. The Figure shows the ZT - CR mix has more resistance in comparison with the CR mix. This is due to the ZT – CR mix absorbing more energy; the lower temperatures used in mixing and compaction may also have helped in this phenomenon. Also, the aggregates have better asphalt coating on them enabling better interlock and performance during testing. The loading rates and crack data are provided in Tables 26-27 found in Appendix C

.

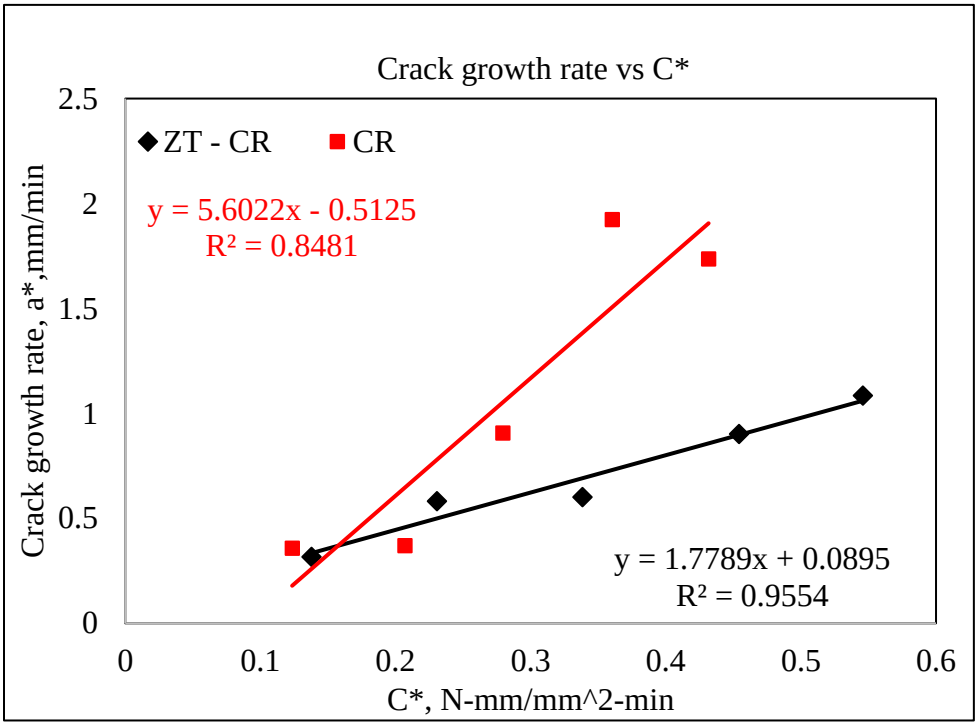

Figure 27. Crack growth rate vs C* comparison

6.5. Fracture Energy Analysis

Analysis of the results thus far indicated that Organosilane modified samples require more energy to fracture due to higher aggregate and asphalt bonds formed by the silane additive. When the load versus time data was compared from IDT results, this phenomenon could not be captured; the simple explanation that the test or loading rate is rater quick. (Figure 28)

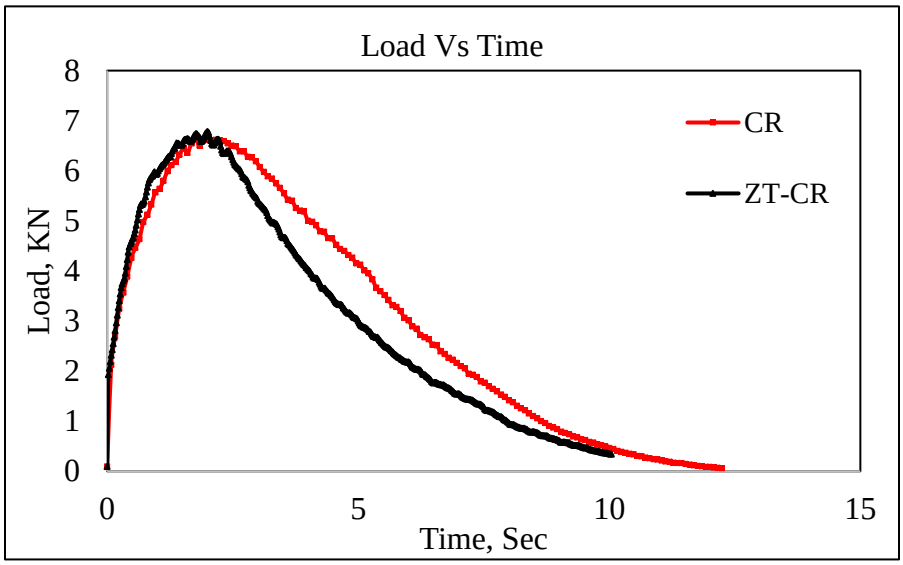

Figure 28. Load Vs Time, IDT test

However, despite that the Organosilane samples require more or similar energy to initiate fracture in specimen, but once the fracture is initiated, it takes more energy for the crack to propagate further in the material due to the bond between asphalt and modified aggregate surface. This was confirmed from the C* fracture test data. It was observed that despite different loading rates, Organosilane modified samples required more energy for

crack propagation (Figure 29). Again, this mechanism was also supported by Figure 27, where crack growth rate is compared against C* parameter.

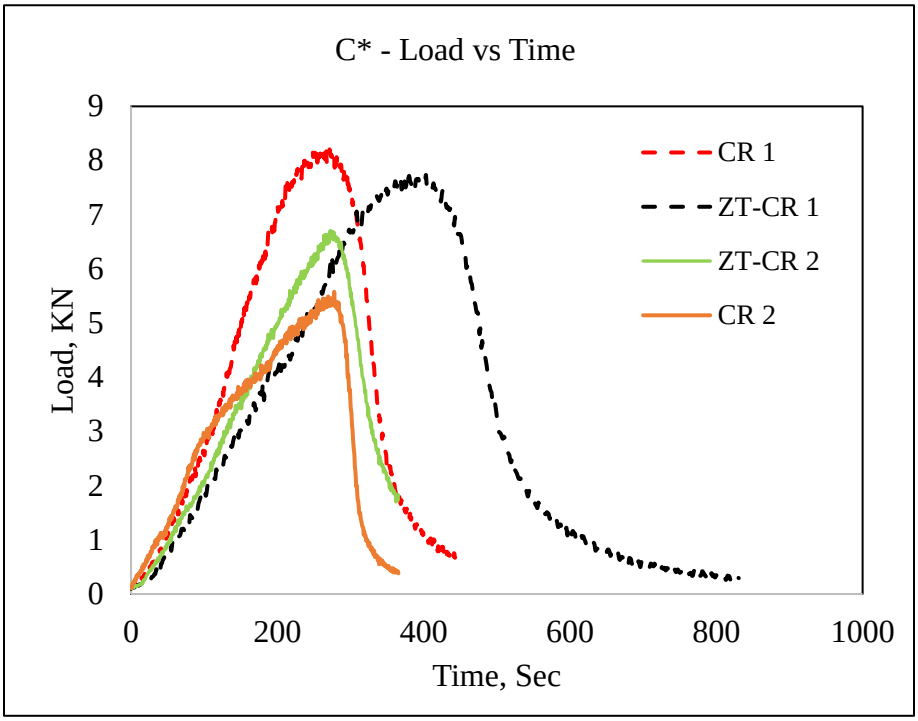

Figure 29. Load vs. Time, C* Test

In Figure 29, CR 1 and ZT- CR 1 represent were subjected to a loading rate of 0.30 mm/min. CR 2 and ZT-CR 2 were subjected to a loading rate of 0.38 mm/min. Irrespective of the loading rates, Organosilane modified mixes required more energy to propagate fracture after the peak load initiated the crack. The graph after the peak load is a gradual downward slope curve for ZT-CR mixes, whereas CR mixes have a steeper downward curve comparatively.

6.6. Compaction Data

One of the other advantages of Organosilane, in addition to lower mixing and compaction temperatures, is the ease of compaction and workability. This could be verified from the Superpave Servopac gyratory compactor data as shown in Figure 30. The ZT-CR mix required less gyrations for same of material to be compacted to same height and air voids content; keeping in mind that the ZT-CR mixed had even a lower mixing and compaction temperature than the CR mix.

On an average, ZT- CR mixes require 12 gyrations less than the CR mixes for same material weight and air void content

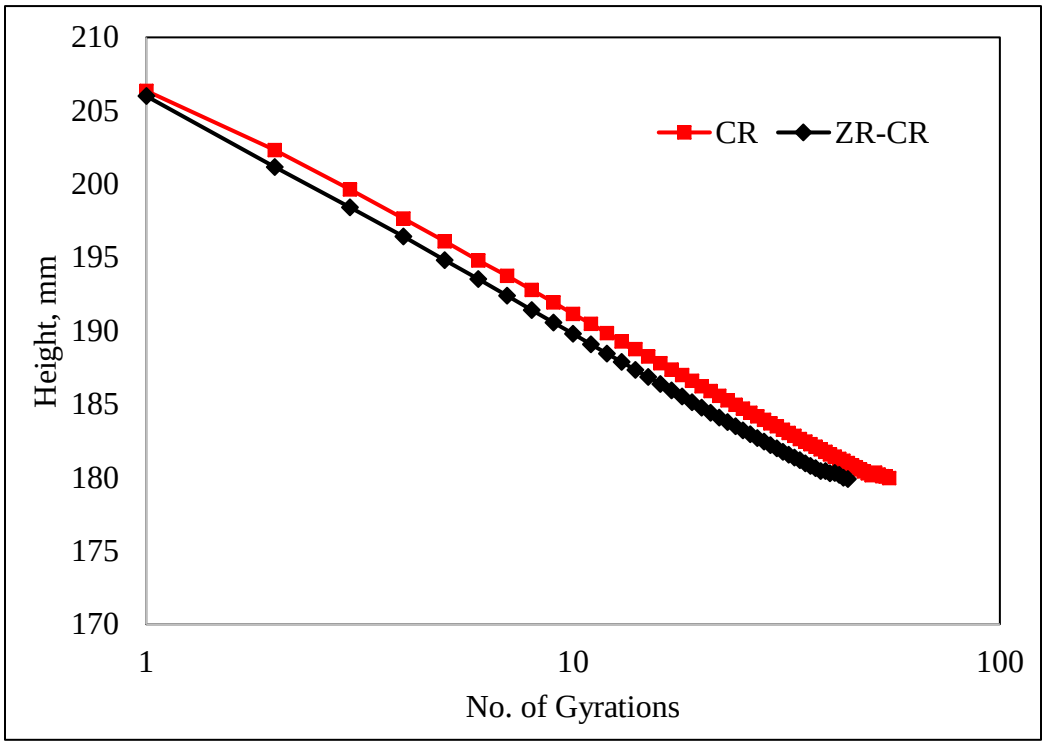

Figure 30. Comparison of compaction effort between mixes

7. STATISTICAL ANALYSIS

Statistical hypothesis tests were performed for the mean and variance of the collected data. The hypothesis was formed from the assumption that the mean values of the CR mix results are equal to the mean values of ZT – CR mixes. The null hypothesis, H was taken as H: $\mu 1 = \mu 2$ and alternate hypothesis, A, A: $\mu 1 \neq \mu 2$. The same process was performed for the variance of results of tests. For analysis of both the mean and the variance, the level of confidence α was chosen appropriately. The hypothesis conditions shown in Figure 31 were obtained from the book, Engineering Statistics, written by A.H Bowker and G.J Lieberman, Feburary 1963.

The tests for which statistical analysis was carried were Dynamic Modulus and Flow Number. The level of acceptance and crtieria are discussed in following sections.

Notation for the Hypothesis H: $\mu_z = \mu_y$	Test Statistic $t' = \frac{\bar{x} - \bar{y}}{\sqrt{\frac{S_z^2}{n_x} + \frac{S_y^2}{n_y}}}$ Formula for Obtaining the Degree of Freedom, ν $\nu = \frac{\left(\frac{S_z^2}{n_x} + \frac{S_y^2}{n_y}\right)^2}{\frac{\left(\frac{S_z^2}{n_x}\right)^2}{n_x + 1} + \frac{\left(\frac{S_y^2}{n_y}\right)^2}{n_y + 1}} - 2$
Criteria for Rejection $\lvert t' \rvert \geq t_{\alpha/2,\nu}$ if we wish to reject when μ_z is not equal to μ_y.	
$t' \geq t_{\alpha,\nu}$ if we wish to reject when $\mu_z > \mu_y$.	
$t' \leq -t_{\alpha,\nu}$ if we wish to reject when $\mu_z < \mu_y$.	

Figure 31. Rejection criteria for the hypothesis assuming when means are equal, and std dev is unknown, Bowker 1963

7.1. Dynamic Modulus

The average values for each frequency and at each temperature was calculates for both mixes. The number of replicates n = 3 was taken. The calculation data is provided in Table 28 – 32. in appendix D

Table 9. Sample of average values for hypothesis testing at -10°C

Temp, ºC	Frequency Hz	E* - ksi		Log E*		Log Red Time, s	
		CR	ZT-CR	CR	ZT-CR	CR	ZT-CR
-10 ºC	25	3724	3463	6.57	6.54	-4.09	-4.62
	10	3532	3354	6.55	6.53	-3.69	-4.22
	5	3445	3258	6.54	6.51	-3.39	-3.92
	1	3324	2994	6.52	6.48	-2.69	-3.22
	0.5	3192	2886	6.50	6.46	-2.39	-2.92
	0.1	2786	2546	6.44	6.41	-1.69	-2.22

The variance of all values for each frequency and at each temperature was calculated for both mixes. The number of replicates n = 3 was taken.

Table 10. Sample of calculated variance values for hypothesis testing at -10°C

Temp, ºC	Frequency Hz	E*- ksi		Log E*		Log Red Time, s	
		CR	ZT-CR	CR	ZT-CR	CR	ZT-CR
-10 ºC	25	26638	12003	0.000	0.000	0.058	0.065
	10	15502	7298	0.000	0.000	0.058	0.065
	5	18808	4013	0.000	0.000	0.058	0.065
	1	24687	6504	0.000	0.000	0.058	0.065
	0.5	21191	9298	0.000	0.000	0.058	0.065
	0.1	5584	8009	0.000	0.000	0.058	0.065

As per Figure 31, the test statistic t' is calculated for every frequency at all temperatures. The terms with notation x denote terms with respect to CR mix and terms with notation y denotes terms with respect to ZT – CR mix.

$$t' = \frac{(\bar{x} - \bar{y})}{\sqrt{\frac{S_x^2}{n_x} + \frac{S_y^2}{n_y}}}$$

Where: $\bar{x}$=Average of CR mix,

$\bar{y}$=Average of ZT – CR mix

S_x^2=Estimate of Variance for CR mix

S_y^2=Estimate of Variance for ZT – CR mix

$n_x = n_y$ =Number of Test Replicates = 3

Table 11. Sample of calculated test statistics for -10°C.

Temp, ºC	Frequency Hz	E* - ksi	Log E*	Log Red Time, s
		t'		
-10 ºC	25	2.296	2.309	2.625
	10	2.044	2.072	2.625
	5	2.145	2.186	2.625
	1	3.243	3.342	2.625
	0.5	3.034	3.094	2.625
	0.1	3.554	3.502	2.625

The degrees of freedom were calculated every frequency at all temperatures.

$$v = \frac{(\frac{S_x^2}{n_x}+\frac{S_y^2}{n_y})^2}{\frac{(\frac{S_x^2}{n_x})^2}{n_{x+1}}+\frac{(\frac{S_y^2}{n_y})^2}{n_{y+1}}} \text{-2}$$

S_x^2=Estimate of Variance for CR mix,

S_y^2=Estimate of Variance for ZT – CR mix

$n_x = n_y$ =Number of Test Replicates = 3

Table 12. Calculated degree of freedom at -10°C

Temp, ºC	Frequency Hz	E* - ksi	Log E*	Log Red Time, s
		Degrees of Freedom		
-10 ºC	25	5.00	5.21	5.97
	10	5.08	5.31	5.97
	5	3.63	3.82	5.97
	1	3.97	4.38	5.97
	0.5	4.94	5.36	5.97
	0.1	5.75	5.42	5.97

To evaluate the tabulated value in which to compare the test statistic, $t_{0.025,\,\nu}$ must be used to locate the value in a standard table of values. The tabulated solutions from the T-table used for comparison of the test statistic are summarized in Table 12.

Table 13. Tabulated t-table values for α = 0.05, at -10°C

Temp, ºC	Frequency Hz	E* - ksi	Log E*	Log Red Time, s
		t table		
-10 ºC	25	2.78	2.57	2.57
	10	2.57	2.57	2.57
	5	3.18	3.18	2.57
	1	3.18	2.78	2.57
	0.5	2.78	2.57	2.57
	0.1	2.57	2.57	2.57

The criteria for rejecting the hypothesis :($\mu 1 = \mu 2$) is as follows. If the null hypothesis is rejected, the alternative :($\mu 1 \neq \mu 2$) must be accepted. Equation which was used to accept or reject the null hypothesis is, $|t'| \geq t_{a/2}, \nu$

The result of Hypothesis testing is shown and summarized in the Table 13. The table displays the result of hypothesis testing, accept being the means of population are same, reject being there are significantly different and not equal.

Table 14. Results of hypothesis tests for the mean of the CR mix to ZT – CR mix

Temp, ºC	Frequency Hz	E* - ksi	Log E*	Log Red Time, s
		Result		
-10 ºC	25	accept	accept	reject
	10	accept	accept	reject
	5	accept	accept	reject
	1	reject	reject	reject
	0.5	reject	reject	reject
	0.1	reject	reject	reject
4.4 ºC	25	accept	accept	reject
	10	accept	accept	reject
	5	accept	accept	reject
	1	accept	accept	reject
	0.5	accept	accept	reject
	0.1	accept	accept	reject
21.1 ºC	25	accept	accept	accept
	10	accept	accept	accept
	5	accept	accept	accept
	1	accept	accept	accept
	0.5	accept	accept	accept
	0.1	accept	accept	accept
37.8 ºC	25	accept	accept	accept
	10	accept	accept	accept
	5	accept	accept	accept
	1	accept	accept	accept
	0.5	accept	accept	accept
	0.1	accept	accept	accept
54.4 ºC	25	accept	accept	accept
	10	accept	accept	accept
	5	accept	accept	accept
	1	accept	accept	accept
	0.5	accept	accept	accept
	0.1	accept	accept	accept

7.2. Flow Number Test

Table 14 to 16 summarize the results of the average values, variances, and test statistic values of all test parameters for the Repeated Load Permanent Deformation tests. The table 16 displays the result of hypothesis testing. All the parameters yielded “Accept” i.e. the means of both populations are same for all parameters tested. There is no significant difference between CR and ZT-CR mixes. The tabulated data is provided in Table 33 in appendix D

Table 15. Average values for hypothesis testing on flow number parameters

Sample	CR	ZT-CR
Flow Number (Cycles)	1434	2151
Resilient Modulus at Failure (Mpa)	744	725
Axial Permanent Strain at Failure εp (%)	1.61	1.34
Axial Resilient Strain at Failure εr (%)	0.05	0.05
εp/εr (%)	31.47	25.03

Table 16. Variance values for hypothesis testing on flow number parameters

Sample	CRMB	ZT
Flow Number (Cycles)	18958	481451
Resilient Modulus at Failure (Mpa)	108	1500
Axial Permanent Strain at Failure εp (%)	0.00305	0.0488
Axial Resilient Strain at Failure εr (%)	1.5556E-06	8E-06
εp/εr (%)	3.33	11.12

Table 17. Results of hypothesis tests for the mean of the CR mix to ZT – CR mix

Sample	DOF	t'	$t_{a/2}, \nu$	Result
Flow Number (Cycles)	1.24	1.76	6.31	accept
Resilient Modulus at Failure (Mpa)	1.43	0.83	12.71	accept
Axial Permanent Strain at Failure εp (%)	1.37	2.07	12.71	accept
Axial Resilient Strain at Failure εr (%)	2.10	1.11	4.30	accept
εp/εr (%)	2.65	2.93	4.30	accept

8. SUMMARY AND CONCLUSIONS

8.1. Summary

Research was initiated and completed to evaluate the effect of Organosilane or Organosilane additive in Crumb Rubber mixes. Both mixes in this study were modified with 20% of Crumb Rubber (CR) by weight of binder. The second mix had a dosage of 0.15 % of Organosilane by weight of virgin binder. A Superpave mix design performed to arrive at the optimum binder content for both mixes. Organosilane enabled lower mixing temperature (by 15 ºC) and required fewer gyrations to compact the specimen to same air void content.

The asphalt mixtures characterization included: Dynamic Modulus Test to evaluate stiffness, Flow Number Test for rutting evaluation, Tensile Strength Ratio to comprehend moisture susceptibility, C* Fracture Test to evaluate crack propagation in the mixes.

8.2. Conclusion

Low E* values at lower temperatures are desirable for resistance to thermal cracking, whereas high E* values at higher temperatures indicate resistance to permanent deformation. The ZT-CR mix had lower dynamic moduli at low temperatures, at higher temperatures the ZT-CR mix had higher moduli in comparison with CR mixes. However, the difference was small and statistical analysis showed the values are not significantly different from each other. The difference in modulus values and slightly higher moduli value could be credited to the better wetting property of the Organosilane.

Due to the formation of silane bond on the surface of the aggregate, the binder is wrapped around the aggregate surface more efficiently than the CR mix, contributing to slightly higher moduli at higher temperatures. In addition, the binder property or role is better retained at higher temperatures in the case of ZT – CR mix.

The flow number test resulted in slightly higher value of flow number for the ZT-CR mix, but again not statistically different from the CR mix. Other flow properties like resilient moduli and strain parameters were statistically same. The ZT-CR had slightly low strain values and had less deformation when compared to CR mixes. This property change could be attributed to better wetting caused by the silane bond but not significant enough to cause in increase in resistance to flow.

Despite lower compaction and mixing temperatures, the ZT-CR retained the properties of CR mixes, a stiffer mix at high temperatures. In general, the ZT-CR mix showed comparable if not better performance than the CR mixes.

The hypothesis was that the formation of silane bond at the surface of aggregate provides effective bonding between the binder and the aggregate surface. This property of Organosilane/Organosilane additive was demonstrated in the moisture susceptibility test. The moisture resistance was increased by 9% over CR mix in case of ZT-CR mixes.

The C* star evaluated the resistance to crack propagation in the mixes at low temperatures. From the plot of crack growth rate, the slope gives the resistance to crack propagation. The ZT-CR mix had roughly 3 times the slope of CR mix conveying better resistance to crack propagation.

This property could be attributed to better bonding in the material due to enhanced silane bond but also the mixture manufactured at lower temperature making the mix better performing in cracking tests. More energy is required to break the bond at the onset of aggregate asphalt phase. This advantage of ZT-CR over CR mixes is very beneficial as they retain the modulus property, resistance to flow, and enhances the moisture susceptibility with increased resistance to crack propagation.

Organosilane additive provides useful reduction in mixing temperature especially for those highly demanded in CR mixes; it also offers better workability at low temperature and less compaction effort as seen from the Gyratory compaction data. The ZT-CR retains the properties of CR mixes in areas of modulus and Flow number, but they offer significant improvement in moisture susceptibility and crack propagation. The added benefit comes without significant change in mix design and binder content, yet better compaction and potential field placement with reduced temperatures. Also, Organosilane potentially reduces any smoke conditions that may be present during the CR mix production.

8.3. Future work

- Evaluation of Organosilane on blending/reaction temperatures of crumb rubber.
- Evaluation the effect of Organosilane when used with pre-activated and reacted crumb rubber and possible reduction of temperatures.
- In depth study of surface tension changes in binder with presence of Organosilane, and effect on properties.
- Stability of Organosilane and susceptibility to asphalt mixture aging.

REFERENCES

AASHTO MP 2 (2001), Standard Specification for Superpave Volumetric Mix Design. Washington, D.C: American Association of State Highway and Transportation Officials.

AASHTO T 283. (2014). Standard Method of Test for Resistance of Compacted Asphalt Mixtures to Moisture-Induced Damage. Washington, D.C: American Association of State Highway and Transportation Officials.

AASHTO TP 107-14 (2016). Standard Method of Test for Determining the Damage Characteristic Curve of Asphalt Mixtures from Direct Tension Cyclic Fatigue Tests. Washington, D.C: American Association of State Highway and Transportation Officials.

AASHTO-T166. (2016). Standard Method of Test for Bulk Specific Gravity (Gmb) of Compacted Hot Mix Asphalt (HMA) Using Saturated Surface-Dry Specimens. Washington, D.C: American Association of State Highway and Transportation Officials.

AASHTO-T209. (2016). Standard Method of Test for Theoretical Maximum Specific Gravity (Gmm) and Density of Hot Mix Asphalt (HMA). Washington, D.C: American Association of State Highway and Transportation Officials.

AASHTO-T342. (2011). Standard Method of Test for Determining Dynamic Modulus of Hot Mix Asphalt (HMA). Washington, D.C: American Association of State Highway and Transportation Officials.

AASHTO-TP79-15. (2016). Standard Method of Test for Determining the Dynamic Modulus and Flow Number for Asphalt Mixtures Using the Asphalt Mixture Performance Tester (AMPT). Washington, D.C: American Association of State Highway and Transportation Officials.

Abdulshafi, O. “Effect of Aggregate on Asphalt Mixture Cracking Using Time Dependent Fracture Mechanics Approach”. Effects of aggregate and Mineral Fillers on Asphalt Mixture Performance,

ASTM STP1147-EB, American Society for Testing and Materials, Philadelphia, 1992

Ajay Ranka, P. M. (2014). Nanotechnology Organosilane Compounds for Chemical Bonding in Road Construction. Asphalt Pavement Technology, 703-716.

Bahia H, Davis R, Effect of Crumb Rubber Modifiers (CRMs) on performance related properties of asphalt binders. AAPT 1994; 1994

Caltrans. (2003). Asphalt rubber usage guide. Office of Flexible Pavement Materials, Sacramento (2003). State of California, Department of Transportation, Materials Engineering and Testing Services.

Cheng, DingXin, Lerose Lane, and R Gary Hicks. "Utilizing warm mix technologies in rubberized asphalt pavements." Asphalt Rubber Conference. Munich, 2012

Copeland, A. (2011). Reclaimed Asphalt Pavement in Asphalt Mixtures: State of Practice. McLean, VA: Federal Highway Administration

Hasan, et al. (2017). Performance Characterizations of Asphalt Binders and Mixtures Incorporating Silane Additive Organosilane. IGNITE-AICCE'17

HMA Mix Design Fundamentals. (2012). Retrieved 03 04, 2018, from Pavement interactive: http://www.pavementinteractive.org/hma-mix-design-fundamentals/

Kamil E. Kaloush, "Asphalt rubber: Performance tests and pavement design issues", ARIZONA STATE UNIVERSITY, 2013.

Kiggundu, R. (1988). Stripping in HMA Mixtures: State of the Art and Critical Reviews of Test Methods. Auburn, AL: National Center for Asphalt Technology

Lieberman, A.H Bowker and G.J G. Lieberman, "Engineering Statistics," February 1963.
M. A. Abdelrahman and S. H. Carpenter, "Mechanism of interaction of asphalt cement with crumb rubber modifier," Transportation Research Record, no. 1661, pp. 106–113, 1999.

Majidzadeh, K., E.M. Kauffmann, D.V. Ramsamooj, and Chan, A.T. (1970). Analysis of Fatigue and Fracture of Bituminous Paving Mixtures, Report No. 2546. U.S. Bureau of Public Roads. Research and Development, 1970.

Mirzababaei, P. (2016). Effect of Organosilane on moisture susceptibility of Warm Mix Asphalt mixtures prepared with different aggregate types and gradations. *Construction and Building Materials , 116*.

NCAT Report 12-09, (2014). Effect of Ground Tire Rubber Particle Size and Grinding Method on Asphalt Binder Properties

Ranka, D. A. (2014). Organo-Silane Nanotechnologies Additives for " Moisture Resistant Asphalt Roads". *AAPT- International Forum.* Atlanta-GA

Raveesh J, M. S. (2017). Laboratory Evaluation ofWMA with Organosilane Warm Mix Additive. International Journal for Research in Applied Science & Engineering Technology, 5(7).

Rohith N, J. R. (2013). A Study on Marshall Stability Properties of Warm Mix Asphalt UsingOrganosilane A Chemicla Additive. International Journal of Engineering Research & Technology, 2(7).

Stempihar J, Kaloush KE (2017) A Notched Disk Crack Propagation Test for Asphalt Concrete. MOJ Civil Eng. 3(5): 00084. DOI: 10.15406/mojce.2017.03.00084

Stempihar, Jeffrey. Development of the C* Fracture Test for Asphalt Concrete Mixtures. Ph.D. Dissertation, Civil and Environmental Engineering, Arizona State University, 2013

Way, George B. "Asphalt-Rubber 45 Years of Progress." Asphalt Rubber. 2012

Willis, J. Richards, Clayton Plemons, Pamela Turner, Carolina Rodezno, and Tyler Mitchell. "Effect of Ground Tire Rubber Particle Size and Grinding Method on Asphalt Binder Properties." National Center for Asphalt Technology, Auburn, 2012.

Witczak, M. W., and Kaloush, K., "Performance Evaluation of Asphalt Modified Mixtures Using Superpave and P-401 Mix Gradings" Maryland Port Administration, Baltimore, Maryland, March 1998

Witczak, M., Kaloush, K., Pellinen, T., El-Bayouny, M., and Von Quintas, H, "Simple Performance Test for Superpave Mix Design," NCHRP 465, 105 pages, Transportation Research Board, National Research Council, National Academy Press, Washington, D.C., 2002.

Zaniewski J, a. V. (2006). Investigation of Moisture Sensitivity of Hot Mix Asphalt. University of West Virginia, Dept. of Civil & Environmental Engineering. Morgantown, WV: Asphalt Technical Program.
Zydex. (2014). *Organosilane-SP Lab Protocol.* Vadodara, India: Zydex Industries.

Zydexindustries. (2015, September 19). *Road Solutions.* Retrieved from Zydex Industries: http://www.zydexindustries.com/roads-products.aspx?key=uORpM5MhoHF4EE/oKvePiw==

APPENDIX

A. MATERIAL PROPERTIES

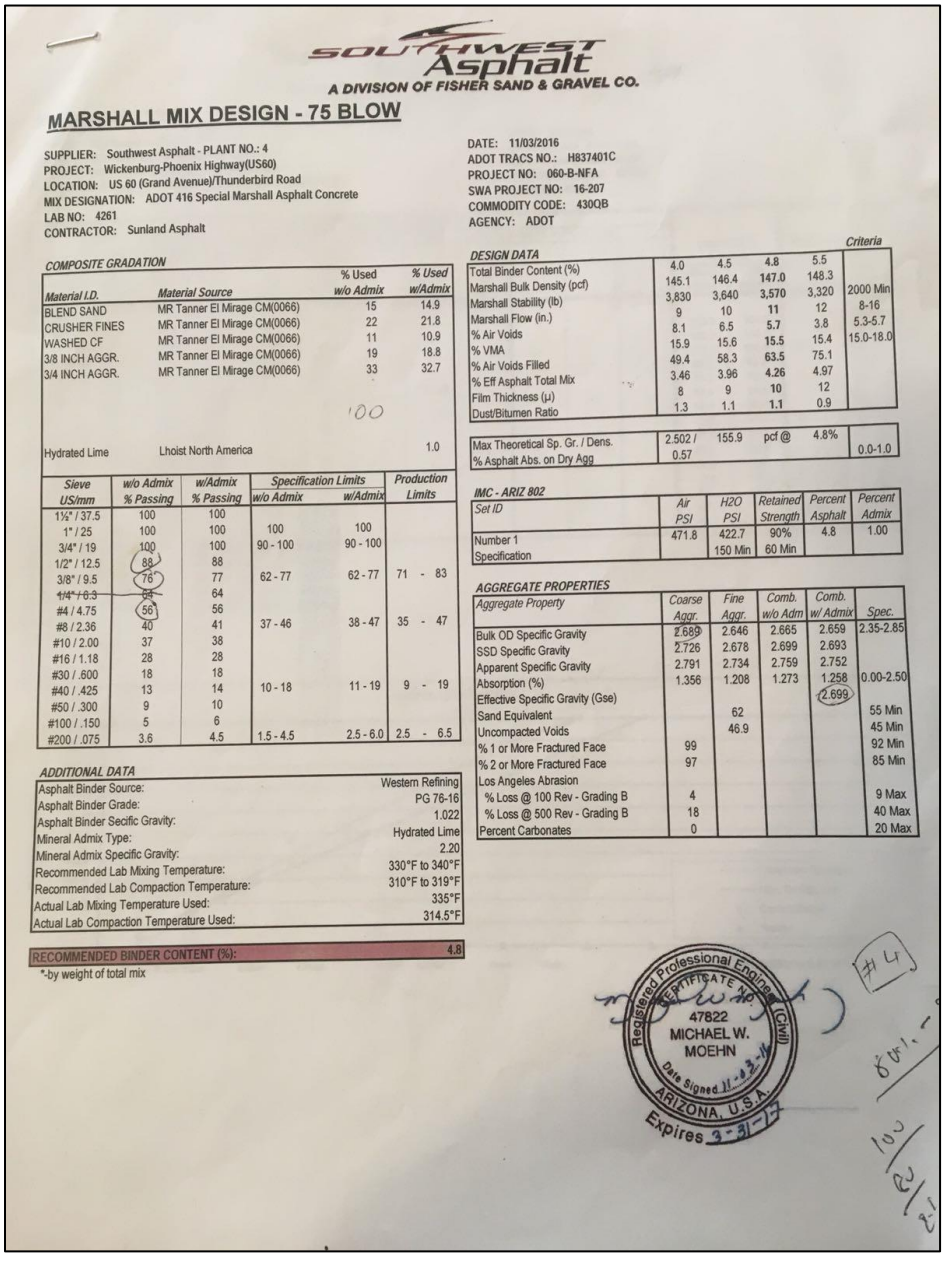

SOUTHWEST Asphalt
A DIVISION OF FISHER SAND & GRAVEL CO.

MARSHALL MIX DESIGN - 75 BLOW

SUPPLIER: Southwest Asphalt - PLANT NO.: 4
PROJECT: Wickenburg-Phoenix Highway(US60)
LOCATION: US 60 (Grand Avenue)/Thunderbird Road
MIX DESIGNATION: ADOT 416 Special Marshall Asphalt Concrete
LAB NO: 4261
CONTRACTOR: Sunland Asphalt

DATE: 11/03/2016
ADOT TRACS NO.: H837401C
PROJECT NO: 060-B-NFA
SWA PROJECT NO: 16-207
COMMODITY CODE: 430QB
AGENCY: ADOT

COMPOSITE GRADATION

Material I.D.	Material Source	% Used w/o Admix	% Used w/Admix
BLEND SAND	MR Tanner El Mirage CM(0066)	15	14.9
CRUSHER FINES	MR Tanner El Mirage CM(0066)	22	21.8
WASHED CF	MR Tanner El Mirage CM(0066)	11	10.9
3/8 INCH AGGR.	MR Tanner El Mirage CM(0066)	19	18.8
3/4 INCH AGGR.	MR Tanner El Mirage CM(0066)	33	32.7
		100	
Hydrated Lime	Lhoist North America		1.0

Sieve US/mm	w/o Admix % Passing	w/Admix % Passing	Specification Limits w/o Admix	Specification Limits w/Admix	Production Limits
1½" / 37.5	100	100			
1" / 25	100	100	100	100	
3/4" / 19	100	100	90 - 100	90 - 100	
1/2" / 12.5	88	88			
3/8" / 9.5	76	77	62 - 77	62 - 77	71 - 83
~~1/4" / 6.3~~	~~64~~	64			
#4 / 4.75	56	56			
#8 / 2.36	40	41	37 - 46	38 - 47	35 - 47
#10 / 2.00	37	38			
#16 / 1.18	28	28			
#30 / .600	18	18			
#40 / .425	13	14	10 - 18	11 - 19	9 - 19
#50 / .300	9	10			
#100 / .150	5	6			
#200 / .075	3.6	4.5	1.5 - 4.5	2.5 - 6.0	2.5 - 6.5

ADDITIONAL DATA

Asphalt Binder Source:	Western Refining
Asphalt Binder Grade:	PG 76-16
Asphalt Binder Secific Gravity:	1.022
Mineral Admix Type:	Hydrated Lime
Mineral Admix Specific Gravity:	2.20
Recommended Lab Mixing Temperature:	330°F to 340°F
Recommended Lab Compaction Temperature:	310°F to 319°F
Actual Lab Mixing Temperature Used:	335°F
Actual Lab Compaction Temperature Used:	314.5°F

RECOMMENDED BINDER CONTENT (%): 4.8
*-by weight of total mix

DESIGN DATA

					Criteria
Total Binder Content (%)	4.0	4.5	4.8	5.5	
Marshall Bulk Density (pcf)	145.1	146.4	147.0	148.3	
Marshall Stability (lb)	3,830	3,640	3,570	3,320	2000 Min
Marshall Flow (in.)	9	10	11	12	8-16
% Air Voids	8.1	6.5	5.7	3.8	5.3-5.7
% VMA	15.9	15.6	15.5	15.4	15.0-18.0
% Air Voids Filled	49.4	58.3	63.5	75.1	
% Eff Asphalt Total Mix	3.46	3.96	4.26	4.97	
Film Thickness (µ)	8	9	10	12	
Dust/Bitumen Ratio	1.3	1.1	1.1	0.9	

Max Theoretical Sp. Gr. / Dens.	2.502 /	155.9	pcf @	4.8%	
% Asphalt Abs. on Dry Agg	0.57				0.0-1.0

IMC - ARIZ 802

Set ID	Air PSI	H2O PSI	Retained Strength	Percent Asphalt	Percent Admix
Number 1	471.8	422.7	90%	4.8	1.00
Specification		150 Min	60 Min		

AGGREGATE PROPERTIES

Aggregate Property	Coarse Aggr.	Fine Aggr.	Comb. w/o Adm	Comb. w/ Admix	Spec.
Bulk OD Specific Gravity	2.689	2.646	2.665	2.659	2.35-2.85
SSD Specific Gravity	2.726	2.678	2.699	2.693	
Apparent Specific Gravity	2.791	2.734	2.759	2.752	
Absorption (%)	1.356	1.208	1.273	1.258	0.00-2.50
Effective Specific Gravity (Gse)				2.699	
Sand Equivalent		62			55 Min
Uncompacted Voids		46.9			45 Min
% 1 or More Fractured Face	99				92 Min
% 2 or More Fractured Face	97				85 Min
Los Angeles Abrasion					
% Loss @ 100 Rev - Grading B	4				9 Max
% Loss @ 500 Rev - Grading B	18				40 Max
Percent Carbonates	0				20 Max

Registered Professional Engineer (Civil)
CERTIFICATE NO.
47822
MICHAEL W.
MOEHN
Date Signed 11-03-16
ARIZONA, U.S.A.
Expires 3-31-17

#4

Figure 32. Aggregate properties – el mirage pit

weight of sample	7050.00		
binder %	6.70	binder weight	472.4
		64-22	377.9
		Crumb Rubber	94.5
		total	472.4
aggregates	6577.7		
gradation of aggregates			
sieve size mm	sieve size in inch	weigth	cumulative
25.00	1.00	0.0	
19.00	3/4	0.0	
12.50	1/2	328.9	6577.7
9.50	3/8	1973.3	6248.8
4.75	#4	2631.1	4275.5
2.36	#8	328.9	1644.4
1.18	#16	263.1	1315.5
0.60	#30	263.1	1052.4
0.30	#50	131.6	789.3
0.15	#100	263.1	657.8
0.08	#200	131.6	394.7
	pan	263.1	263.1
		6577.7	

Figure 33. Gap gradation for CR mix

weight of sample	7050.00		
binder %	6.80	binder weight	479.4
		64-22	383.5
		Crumb Rubber	95.9
		total	479.4
aggregates	6570.6		
gradation of aggregates			
sieve size mm	sieve size in inch	weigth	cumulative
25.00	1.00	0.0	
19.00	3/4	0.0	
12.50	1/2	328.5	6570.6
9.50	3/8	1971.2	6242.1
4.75	#4	2628.2	4270.9
2.36	#8	328.5	1642.7
1.18	#16	262.8	1314.1
0.60	#30	262.8	1051.3
0.30	#50	131.4	788.5
0.15	#100	262.8	657.1
0.08	#200	131.4	394.2
	pan	262.8	262.8
		6570.6	

Figure 34. Gap gradation for ZT – CR mix

APPENDIX

B. SUPERPAVE MIX DESIGN CALCULATIONS

Table 18. Gmb calculations – CR Mix

Binder Percent (%)	Gmm	Mass in air (A) Gm	Mass SSD (C) gm	Mass in water (B) gm	Gmb $\frac{A}{B-C}$	% Air Voids $(1 - \frac{Gmb}{Gmm})*100$
6.50	2.45	4699.4	2711.4	4725.8	2.34	4.9%
6.50	2.45	4701.1	2720.7	4726.7	2.34	4.5%
7.00	2.43	4698	2713.6	4713.8	2.35	3.3%
7.00	2.43	4702	2716.6	4713.1	2.36	2.9%
7.50	2.41	4697.3	2705.2	4703.3	2.35	2.5%
7.50	2.41	4698.5	2710.5	4706.8	2.35	2.5%

Table 19. Final volumetric properties – CR Mix

Pb (%)	% Air Voids	% VMA	% VFA	%Gmm	%Gmm	D.P.
				$N_{initial}$	N_{max}	
6.5	4.7	17.71719	73.47209	86.9	97.3	0.6
7	3.1	17.63257	82.4189	87.1	97.4	0.7
7.5	2.5	18.24934	86.30088	87.4	97.3	0.7

Table 20. Gmb calculations – ZT - CR Mix

Binder Percent (%)	Gmm	Mass in air (A) gm	Mass SSD (C) gm	Mass in water (B) gm	Gmb $\frac{A}{B-C}$	% Air Voids $(1 - \frac{Gmb}{Gmm})*100$
6.5	2.45	4706.5	4743	2718.9	2.33	4.5%
6.5	2.45	4707.1	4744.3	2719.1	2.32	4.5%
7	2.43	4704.6	4724.6	2711.1	2.34	3.7%
7	2.43	4704.1	4722.6	2710.7	2.34	3.7%
7.5	2.41	4702.2	4722	2702.4	2.33	3.3%

Table 21. Final volumetric properties – ZT- CR Mix

Pb (%)	% Air Voids	% VMA	% VFA	%Gmm $N_{initial}$	%Gmm N_{max}	D.P.
6.5	4.51	17.89	74.79	87.4	97	0.6
7	3.7	18.16	79.62	87.5	97	0.6
7.5	3.32	18.95	82.48	87.7	97.1	0.7

Volumetric property curves for 6.7% CR mix from superpave mix design:

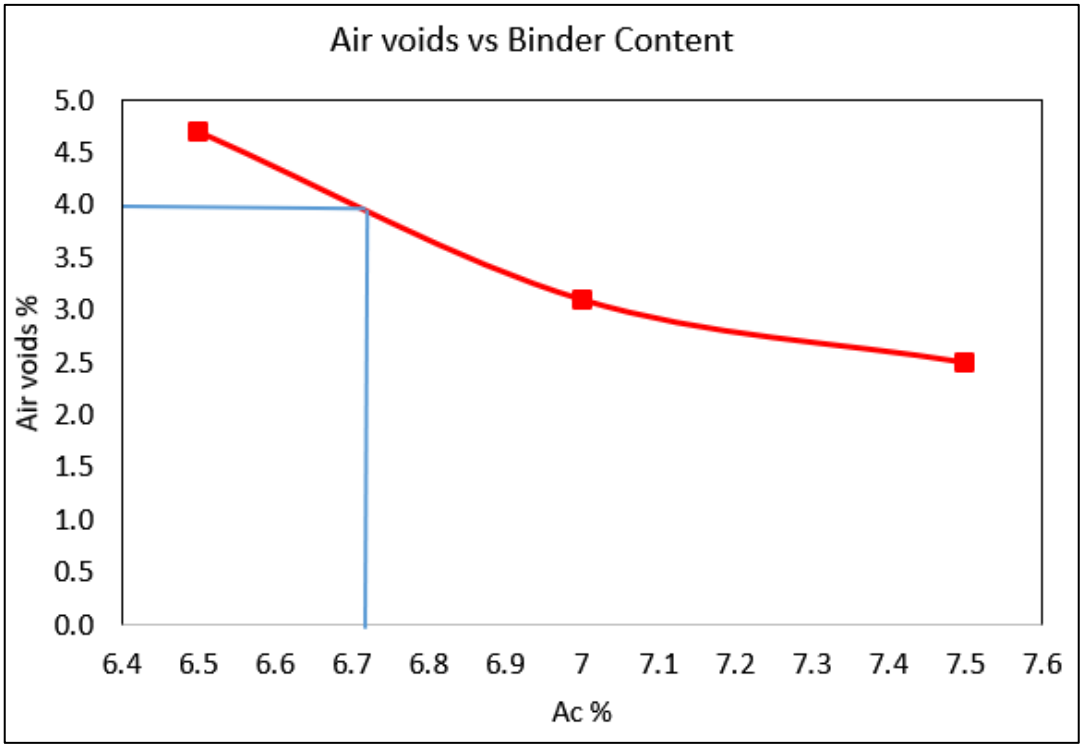

Figure 35. Air voids % vs asphalt content % - CR mix

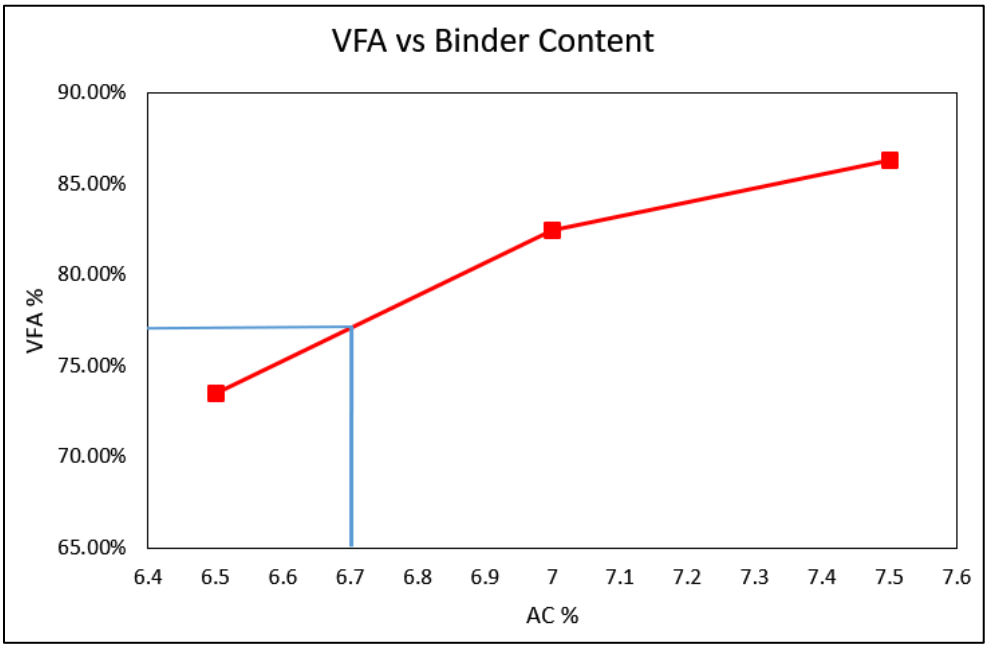

Figure 36. % VFA % vs asphalt content % - CR mix

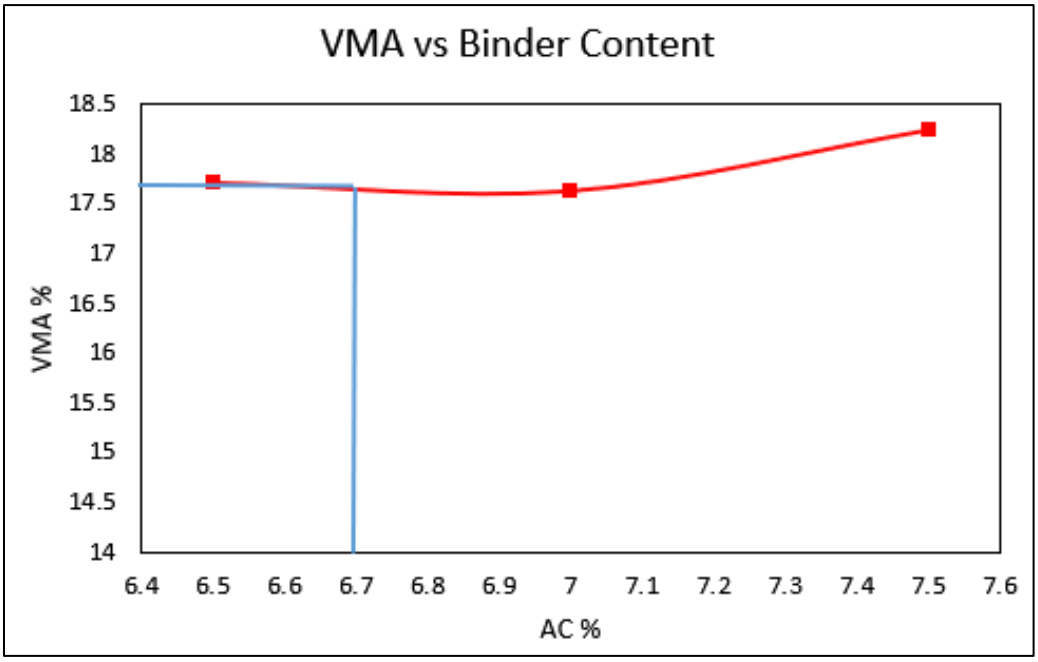

Figure 37. % VMA vs asphalt Content % - CR mix

Volumetric Property Curves for 6.8% ZT- CR Mix from Superpave Mix Design:

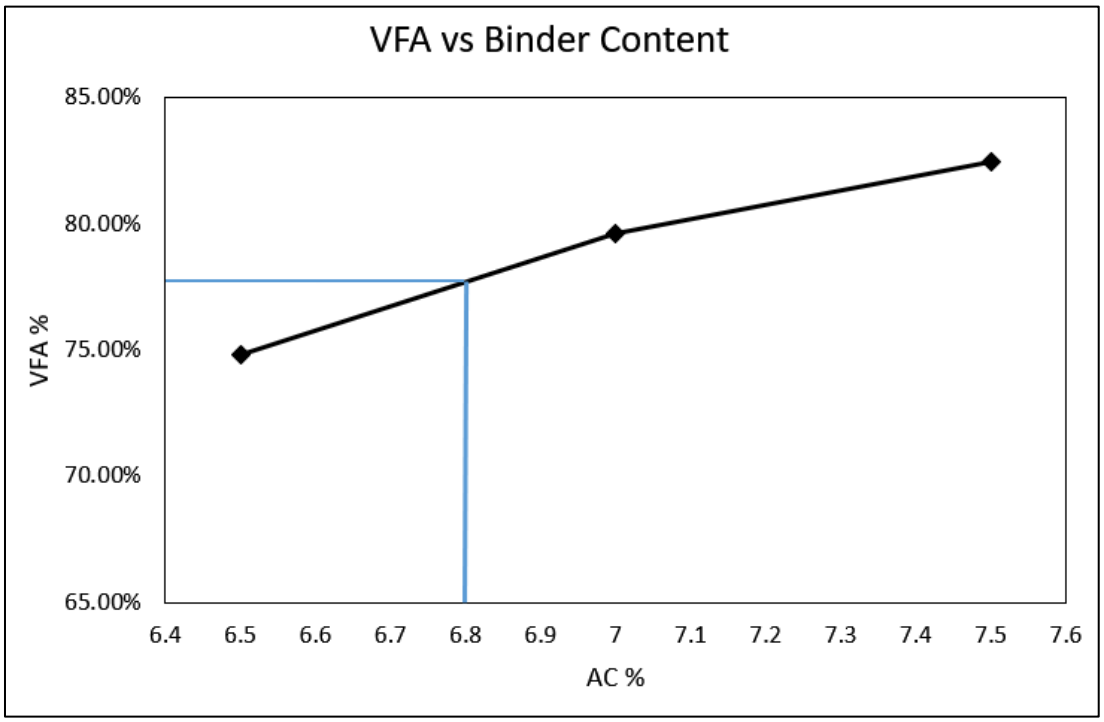

Figure 38. % VFA % vs asphalt Content %, ZT- CR mix

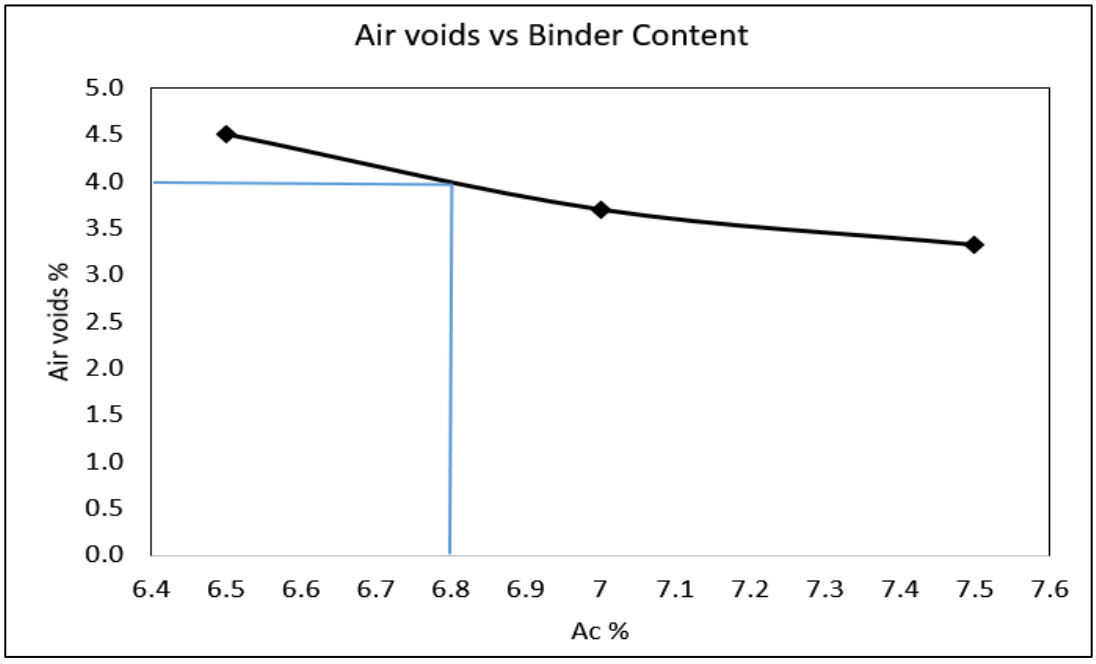

Figure 39. Air Voids % vs asphalt Content %, ZT- CR mix

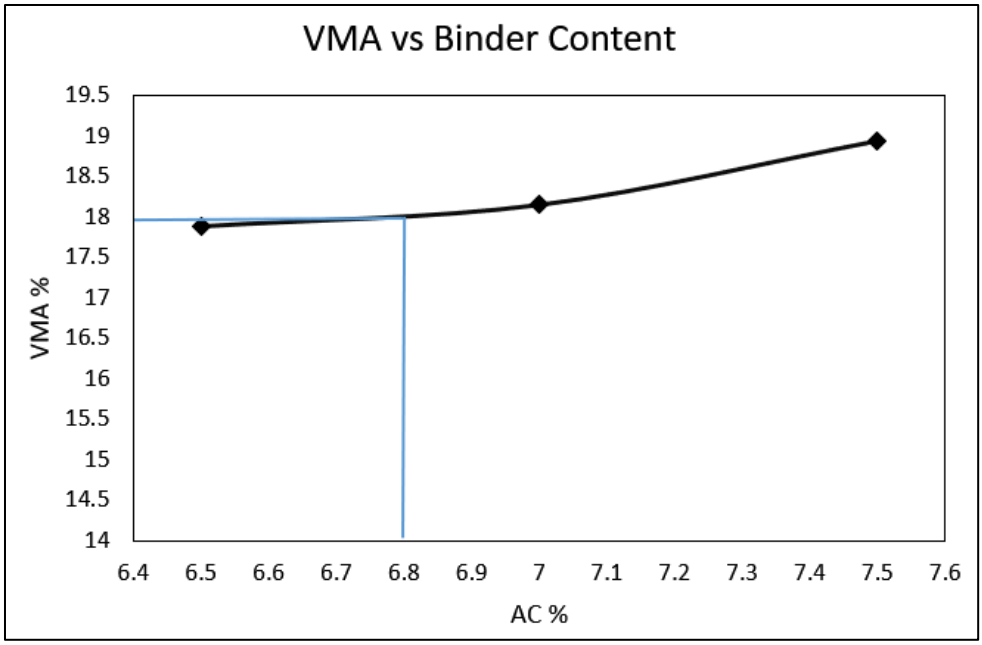

Figure 40. % VMA vs asphalt Content %, ZT - CR mix

APPENDIX

C. RESULTS OF LABORATOTRY TESTING

Figure 41. Dynamic modulus sample LVDT instrumentation 120° apart

Table 22. Dynamic modulus |E*| for CR mix

Temperature (℃)	Frequency (Hz)	Dynamic Modulus, |E*| ksi				
		Replicate 1	Replicate 2	Replicate 3	Average	Std. Dev.
-10	25	3795.64	3839.08	3537.18	3723.96	133.26
-10	10	3488.16	3672.21	3434.93	3531.76	101.66
-10	5	3430.87	3588.74	3315.56	3445.06	111.98
-10	1	3178.79	3303.31	3490.91	3324.34	128.29
-10	0.5	3060.88	3165.52	3348.49	3191.63	118.86
-10	0.1	2756.30	2729.83	2870.44	2785.52	61.01
4.4	25	2272.60	2820.55	2273.61	2455.58	258.07
4.4	10	2093.18	2460.42	2108.56	2220.72	169.61
4.4	5	1936.11	2261.14	1981.07	2059.44	143.80
4.4	1	1597.59	1888.54	1670.40	1718.84	123.62
4.4	0.5	1474.60	1756.41	1557.99	1596.33	118.20
4.4	0.1	1222.09	1446.17	1287.79	1318.68	94.05
21,1	25	1193.81	1353.64	1277.49	1274.98	65.28
21,2	10	1067.48	1190.76	1166.68	1141.64	53.35
21,3	5	962.76	1074.15	1057.18	1031.36	49.00
21,4	1	704.45	817.00	764.49	761.98	45.98
21,5	0.5	603.07	721.13	675.44	666.54	48.61
21,6	0.1	421.04	520.25	491.97	477.75	41.73
37.8	25	507.34	623.81	611.48	580.88	52.24
37.8	10	423.66	513.87	499.07	478.87	39.50
37.8	5	353.75	442.22	422.93	406.30	37.99
37.8	1	224.23	273.69	268.32	255.41	22.16
37.8	0.5	192.03	229.88	223.65	215.19	16.57
37.8	0.1	132.71	152.87	149.53	145.04	8.82
54.4	25	202.33	240.18	231.19	224.57	16.15
54.4	10	160.85	183.62	185.21	176.56	11.13
54.4	5	134.01	148.08	150.40	144.17	7.24
54.4	1	87.75	92.68	92.82	91.08	2.36
54.4	0.5	76.14	77.16	76.29	76.53	0.45
54.4	0.1	56.71	53.08	52.50	54.10	1.86

Table 23. Dynamic modulus |E*| for ZT - CR Mix

Temperature (℃)	Frequency (Hz)	Dynamic Modulus, |E*| ksi				
		Replicate 1	Replicate 2	Replicate 3	Average	Std. Dev.
-10	25	3440.58	3367.05	3582.58	3463.40	89.46
-10	10	3438.84	3267.99	3353.92	3353.59	69.75
-10	5	3317.30	3191.26	3265.45	3258.01	51.72
-10	1	3062.91	2905.11	3012.94	2993.65	65.85
-10	0.5	2976.61	2784.58	2895.97	2885.72	78.73
-10	0.1	2596.17	2443.02	2599.80	2546.33	73.07
4.4	25	2497.11	2613.87	3002.28	2704.42	215.94
4.4	10	2377.75	2399.36	2774.28	2517.13	182.05
4.4	5	2238.51	2255.77	2592.11	2362.13	162.77
4.4	1	1875.92	1904.35	2165.27	1981.84	130.22
4.4	0.5	1732.91	1783.96	2024.73	1847.20	127.25
4.4	0.1	1441.67	1468.80	1668.80	1526.43	101.28
21,1	25	1317.23	1301.28	1489.83	1369.45	85.37
21,2	10	1168.13	1133.32	1299.68	1200.38	71.64
21,3	5	1046.16	1015.70	1183.65	1081.84	73.06
21,4	1	763.77	745.78	886.18	798.58	62.38
21,5	0.5	669.78	652.09	781.75	701.21	57.41
21,6	0.1	482.83	460.93	594.80	512.85	58.63
37.8	25	660.94	567.82	696.76	641.84	54.34
37.8	10	540.56	456.14	582.33	526.34	52.49
37.8	5	466.44	393.49	502.70	454.21	45.42
37.8	1	308.64	250.63	337.50	298.92	36.13
37.8	0.5	261.79	209.14	286.88	252.61	32.40
37.8	0.1	174.34	142.43	197.54	171.43	22.59
54.4	25	252.37	209.87	259.47	240.57	21.90
54.4	10	206.53	163.17	207.84	192.51	20.76
54.4	5	173.03	130.82	171.00	158.28	19.44
54.4	1	107.47	79.77	112.84	100.03	14.49
54.4	0.5	90.36	65.70	93.11	83.06	12.32
54.4	0.1	62.51	44.96	67.73	58.40	9.74

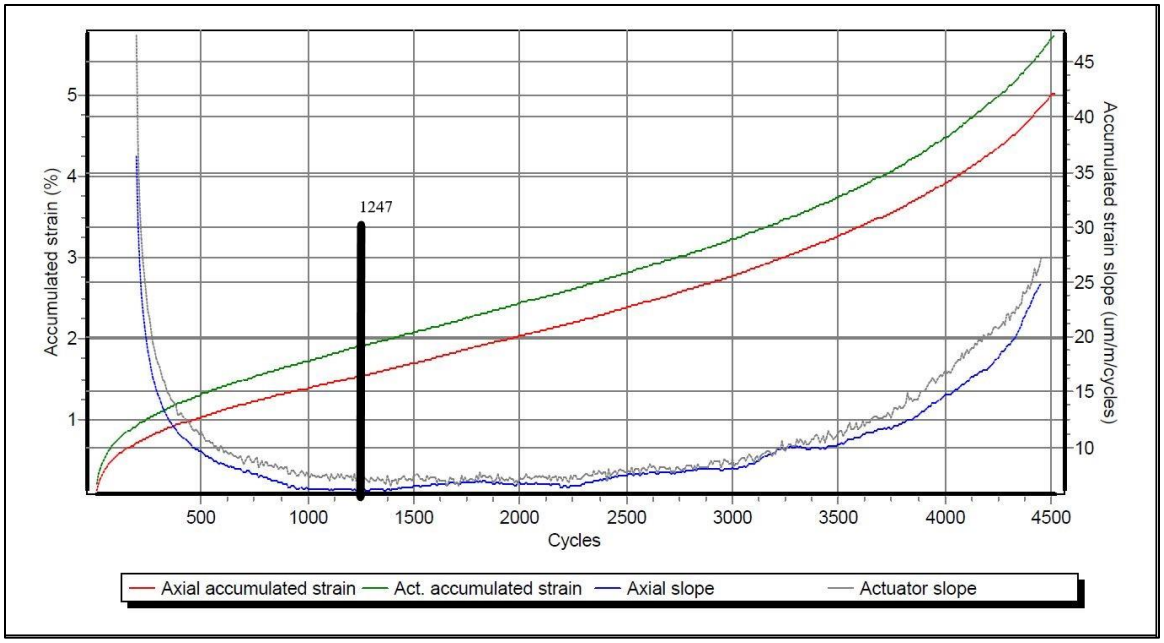

Figure 42. Accumulated strain vs number of cycles for rep 1 – CR mix

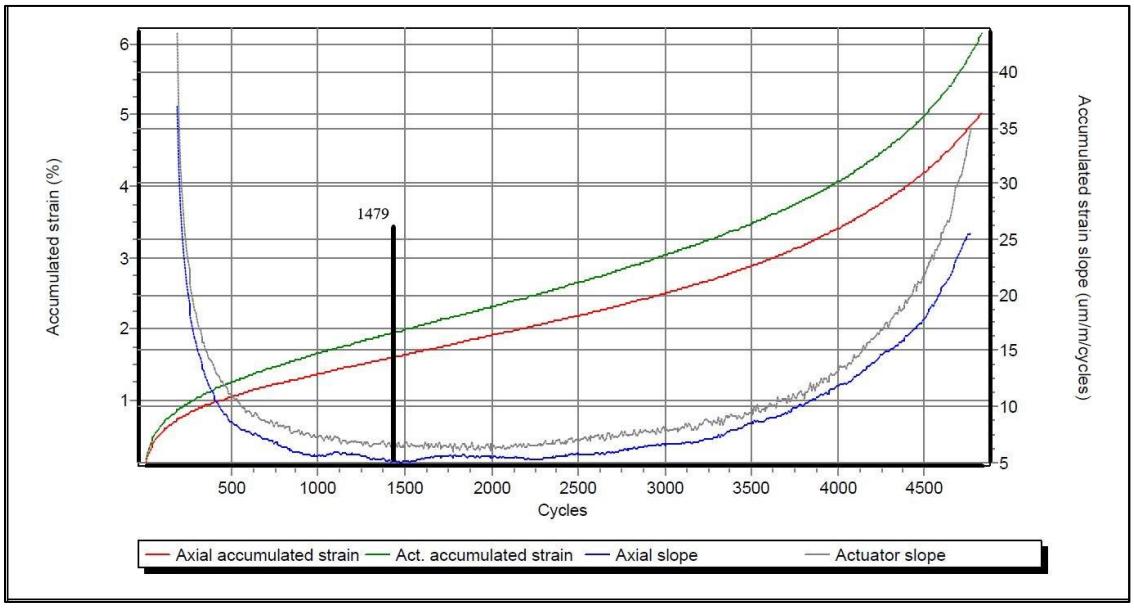

Figure 43. Accumulated strain vs number of cycles for rep 2 – CR mix

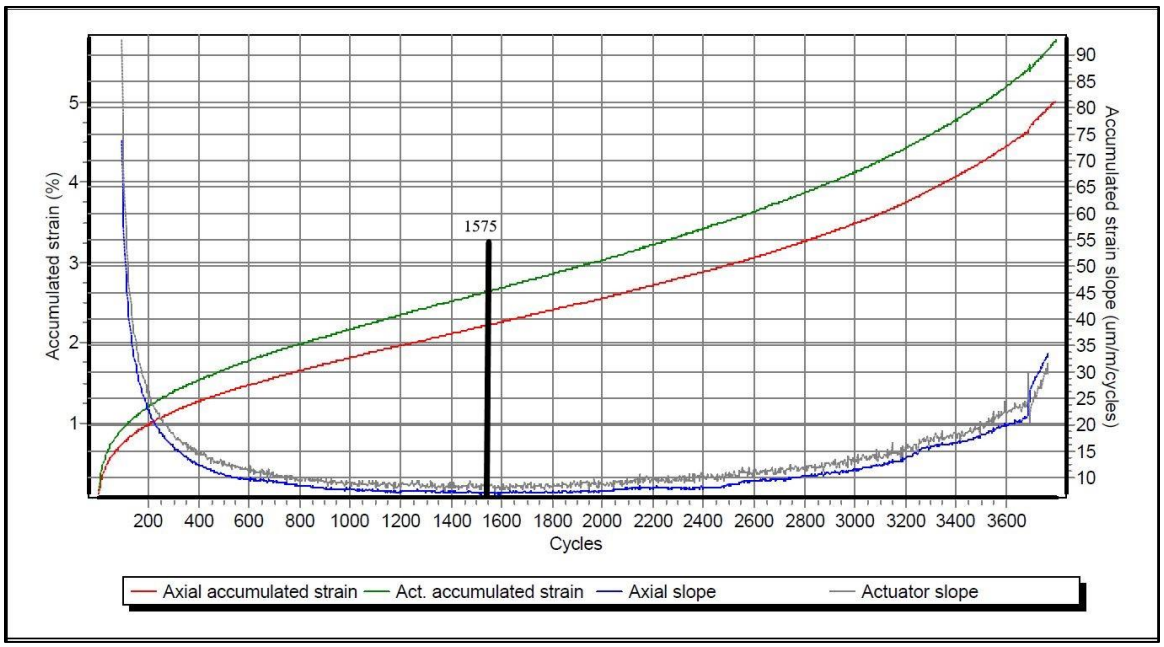

Figure 44. Accumulated strain vs number of cycles for rep 3 – CR mix

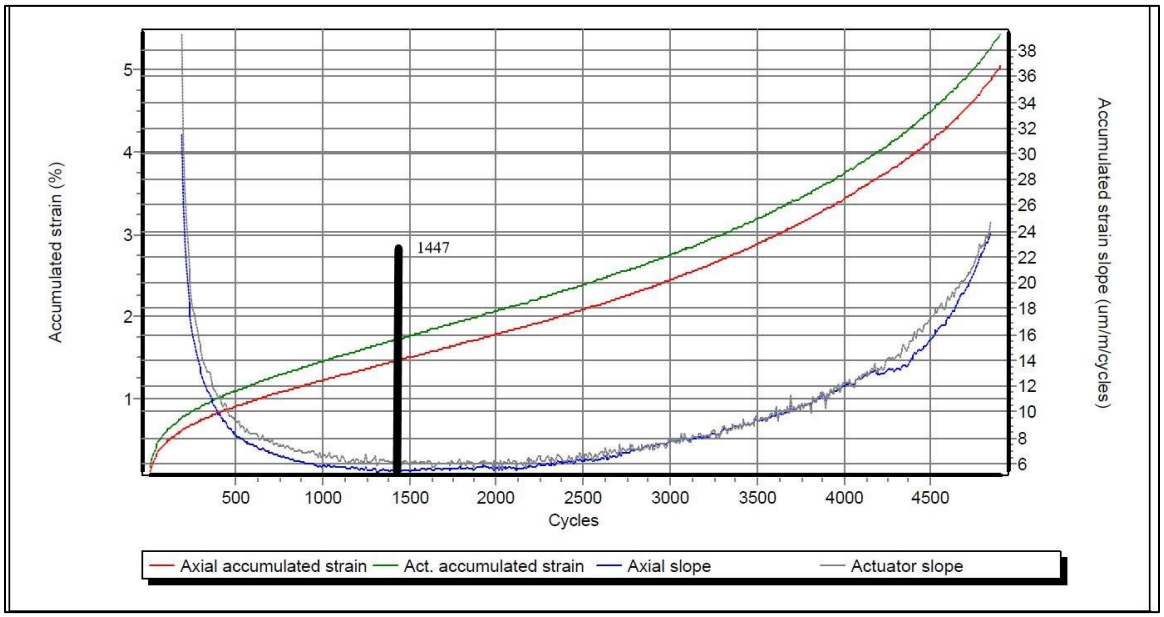

Figure 45. Accumulated strain vs number of cycles for rep 1, ZT – CR mix

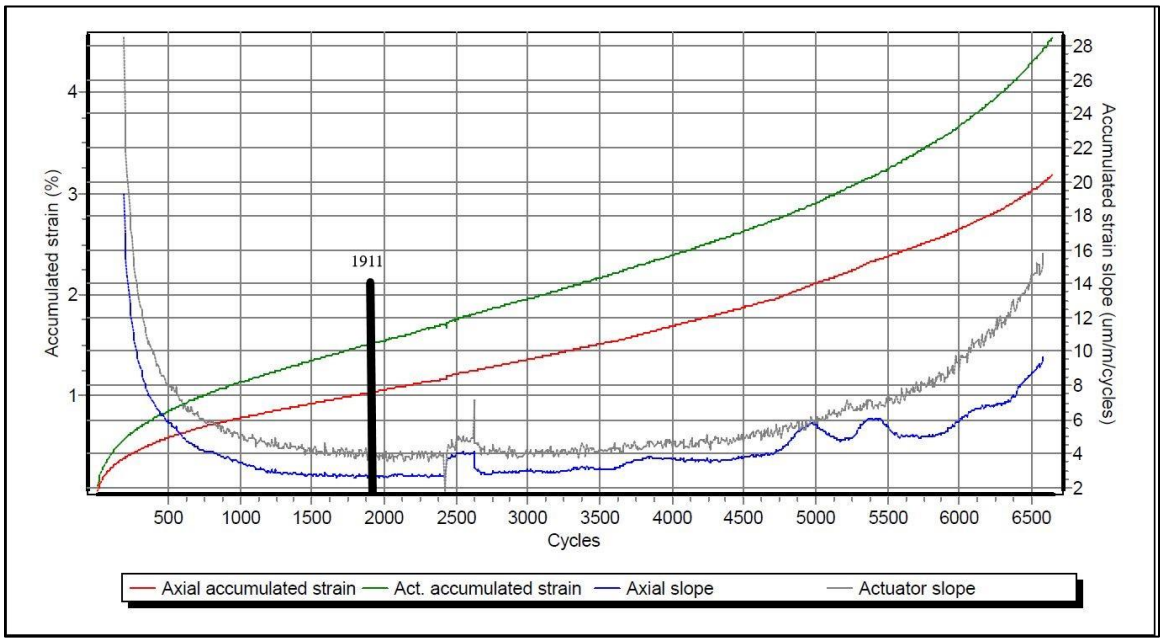

Figure 46. Accumulated strain vs number of cycles for rep 2, ZT – CR mix

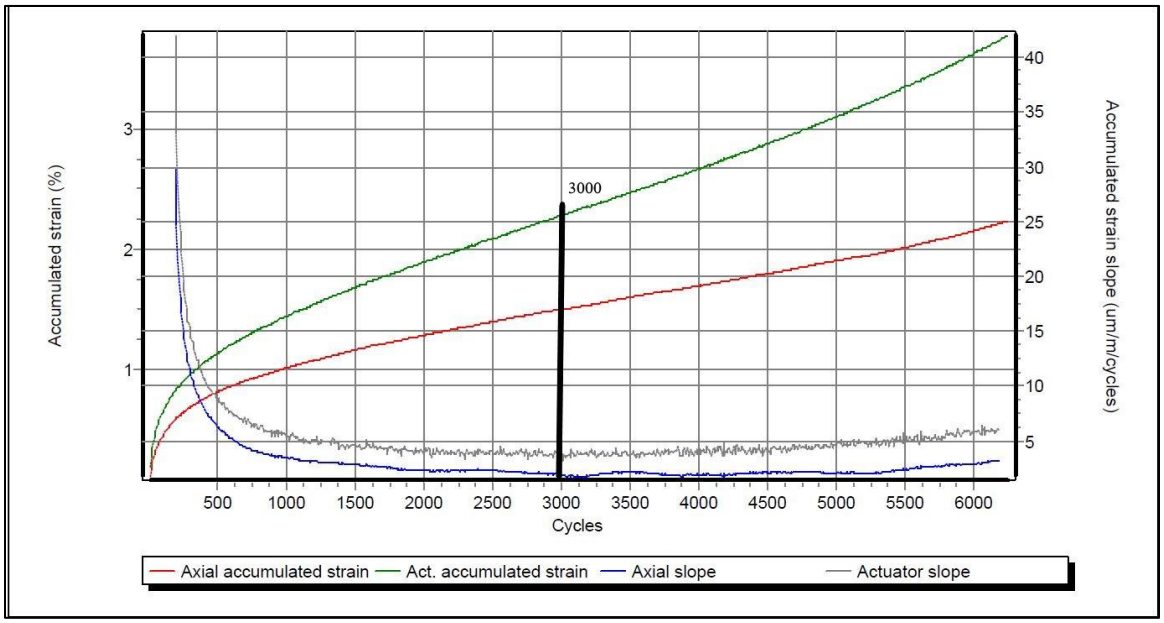

Figure 47. Accumulated strain vs number of cycles for rep 3, ZT – CR mix

Figure 48. TSR sample testing setup

Table 24. TSR data for CR Mix

Condition		WET SUBSET			DRY SUBSET		
Sample identification		1	3	5	2	4	6
		1c	3c	5c	2c	4c	6c
Diameter, mm (in.)	D	99	99.2	99.3	99.2	99	99.3
Thickness, mm (in.)	t	62.8	67.3	64.1	61.3	61.2	63.4
Dry mass in air, g	A	1092.8	1174.1	1121.6	1074.6	1038.4	1112.5
SSD mass, g	B	1098.1	1184.5	1128.3	1082.4	1046.2	1116.8
Mass in water, g	C	622.9	670.7	639.4	615.1	589.9	633.4
Volume (B – C), cm3	E	475.2	513.8	488.9	467.3	456.3	483.4
Bulk specific gravity (A/E)	Gmb	2.30	2.29	2.29	2.30	2.28	2.30
Maximum specific gravity	Gmm	2.44	2.44	2.44	2.44	2.44	2.44
% air voids [100(Gmm – Gmb)/Gmm]	Pa	5.75	6.35	5.98	5.75	6.73	5.68
Average % air voids	%	6.03			6.06		
Volume of air voids (PaE/100), cm3	Va	27.331	32.611	29.228	26.890	30.726	27.457
Load, N (lbf)	P				10242	7877	9281
Saturated		min @					
Thickness, mm (in.)	t'	64.01	65.67	63.67			
SSD mass, g	B'	1112.4	1197.2	1142.3			
Volume of absorbed water (B' – A), cm3	J'	19.6	23.1	20.7			
Load, N (lbf)	P'	6427	7590	6250			
% saturation (100J'/Va)	S'	71.7	70.8	70.8			
Dry strength [2000P/πtD (2P/πtD)], kPa (psi)	S1				1072.2	827.7	938.5
Wet strength [2000P'/πt'D (2P/πt'D)], kPa (psi)	S2	645.7	741.7	629.3			
Average tensile strenght Dry subset, kPa	S1avg				946.1		
Average tensile strenght Wet subset, kPa	S2avg	672.2					
TSR (S2/S1)		71%					

Table 25. TSR data for ZT- CR Mix

Condition		WET SUBSET			DRY SUBSET		
Sample identification		1	2	3	4	5	3
		1z	2z	3z	4z	5z	6z
Diameter, mm (in.)	D	99.2	99.2	99.3	99.2	99	99
Thickness, mm (in.)	t	60.6	62.7	61.6	66.7	62.7	63.5
Dry mass in air, g	A	1052.7	1115.6	1042.7	1174.8	1093.5	1074.3
SSD mass, g	B	1061	1123.2	1055.5	1183.2	1101.4	1091.8
Mass in water, g	C	601.4	636.1	595.6	668.4	623.5	620.7
Volume (B – C), cm3	E	459.6	487.1	459.9	514.8	477.9	471.1
Bulk specific gravity (A/E)	Gmb	2.29	2.29	2.27	2.282	2.288	2.280
Maximum specific gravity	Gmm	2.430	2.430	2.430	2.430	2.430	2.430
% air voids [100(Gmm – Gmb)/Gmm]	Pa	5.742	5.749	6.698	6.088	5.838	6.156
Average % air voids	%	6.06			6.03		
Volume of air voids (PaE/100), cm3	Va	26.390	28.005	30.805	31.343	27.900	29.001
Saturated		min @					
Thickness, mm (in.)	t'	61	63	61.67			
SSD mass, g	B'	1073.2	1135.3	1065.1			
Volume of absorbed water (B' – A), cm3	J'	20.5	19.7	22.4			
Load, N (lbf)	P'	7117	8795	4480			
% saturation (100J'/Va)	S'	77.7	70.3	72.7			
Dry strength [2000P/πtD (2P/πtD)], kPa (psi)	S1				913.2	1028.5	711.8
Cracked/broken aggregate?							
Average tensile strenght Dry subset, kPa	S1avg				884.5		
Average tensile strenght Wet subset, kPa	S2avg	703.5					
TSR (S2/S1)		80%					

Table 26. Summary of C* fracture test results for CR Mix

Sample ID:		Average Thickness, b (mm):	Displacement Rate, Δ* (mm/min) :	
sample CS7		49.67	0.150	
Crack Length,	Time T, (Min)	Force (KN)	Force per Unit	Crack Growth
10.00	9.33	4.730	95.23	
20.00	9.60	4.510	90.80	
30.00	10.25	3.400	68.45	
40.00	10.58	2.660	53.55	
50.00	11.03	2.030	40.87	**0.358**
60.00	11.40	1.680	33.82	
70.00	11.75	1.350	27.18	
80.00	12.07	1.110	22.35	
90.00	13.83	0.880	17.72	
Sample ID:		**Average Thickness, b (mm):**	**Displacement Rate, Δ* (mm/sec) :**	
Sample CS6		**48.67**	**0.228**	
10.00	5.80	5.510	113.21	
20.00	6.03	5.420	111.36	
30.00	6.53	5.210	107.05	
40.00	6.62	5.160	106.02	
50.00	6.70	5.060	103.97	**0.369**
60.00	7.33	4.160	85.47	
70.00	8.03	3.160	64.93	
80.00	9.27	1.920	39.45	
90.00	10.25	1.310	26.92	

Sample ID:		Average Thickness, b (mm):	Displacement Rate, Δ* (mm/sec) :	
Sample CS2		50.00	0.300	
10.00	7.90	5.200	104.00	
20.00	8.17	3.830	76.60	
30.00	8.25	3.510	70.20	
40.00	8.35	3.190	63.80	
50.00	8.43	2.900	58.00	**0.906**
60.00	8.83	2.130	42.60	
70.00	9.18	1.700	34.00	
80.00	9.38	1.520	30.40	
90.00	9.67	1.360	27.20	

Sample ID:		Average Thickness, b (mm):	Displacement Rate, Δ* (mm/sec) :	
Sample CS4		48.00	0.378	
10.00	4.47	5.450	113.54	
20.00	4.53	5.370	111.88	
30.00	4.60	5.330	111.04	
40.00	4.68	5.280	110.00	
50.00	4.77	5.110	106.46	**1.923**
60.00	4.93	4.170	86.88	
70.00	5.03	3.110	64.79	
80.00	5.17	1.720	35.83	
90.00	5.33	1.070	22.29	

Sample ID:		Average Thickness, b (mm):	Displacement Rate, Δ* (mm/sec) :	
Sample CS5		55.33	0.450	
10.00	3.50	4.300	77.72	
20.00	3.77	3.660	66.15	
30.00	3.90	3.224	58.27	
40.00	4.00	2.634	47.61	
50.00	4.07	2.239	40.47	**1.735**
60.00	4.13	1.759	31.79	
70.00	4.18	1.451	26.22	
80.00	4.25	0.989	17.87	
90.00	4.33	0.772	13.95	

Table 27. Summary of C* fracture test results for ZT-CR Mix

Sample ID:		Average Thickness, b (mm):	Displacement Rate, Δ* (mm/min) :	
sample CS7		49.67	0.150	
Crack Length,	Time T, (Min)	Force (KN)	Force per Unit	Crack Growth
10.00	9.33	4.730	95.23	
20.00	9.60	4.510	90.80	
30.00	10.25	3.400	68.45	
40.00	10.58	2.660	53.55	
50.00	11.03	2.030	40.87	**0.358**
60.00	11.40	1.680	33.82	
70.00	11.75	1.350	27.18	
80.00	12.07	1.110	22.35	
90.00	13.83	0.880	17.72	
Sample ID:		**Average Thickness, b (mm):**	**Displacement Rate, Δ* (mm/sec) :**	
Sample CS6		**48.67**	**0.228**	
10.00	5.80	5.510	113.21	
20.00	6.03	5.420	111.36	
30.00	6.53	5.210	107.05	
40.00	6.62	5.160	106.02	
50.00	6.70	5.060	103.97	**0.369**
60.00	7.33	4.160	85.47	
70.00	8.03	3.160	64.93	
80.00	9.27	1.920	39.45	
90.00	10.25	1.310	26.92	

Sample ID:		Average Thickness, b (mm):	Displacement Rate, Δ* (mm/sec) :	
zs5		47.67	0.228	
10.00	5.75	5.225	109.60	
20.00	6.13	4.352	91.29	
30.00	6.37	2.887	60.56	
40.00	6.58	2.020	42.38	
50.00	6.83	1.465	30.73	0.582
60.00	7.17	1.047	21.96	
70.00	7.63	0.842	17.67	
80.00	8.22	0.592	12.42	
90.00	8.63	0.487	10.21	
Sample ID:		**Average Thickness, b (mm):**	**Displacement Rate, Δ* (mm/sec) :**	
zs2		**53.00**	**0.300**	
10.00	4.65	8.014	151.21	
20.00	5.02	7.309	137.91	
30.00	5.33	5.859	110.56	
40.00	5.50	4.465	84.24	
50.00	5.65	3.302	62.30	0.600
60.00	5.77	2.695	50.84	
70.00	5.95	2.097	39.56	
80.00	6.33	1.401	26.43	
90.00	7.17	0.800	15.09	
Sample ID:		**Average Thickness, b (mm):**	**Displacement Rate, Δ* (mm/sec) :**	
ZS3		**46.33**	**0.378**	
10.00	3.30	5.713	123.31	
20.00	3.42	4.746	102.43	
30.00	3.63	3.416	73.73	
40.00	3.83	2.795	60.34	
50.00	4.23	1.938	41.83	0.901
60.00	4.45	1.654	35.70	
70.00	4.70	1.486	32.08	
80.00	4.95	1.278	27.58	
90.00	5.22	1.138	24.57	
Sample ID:		**Average Thickness, b (mm):**	**Displacement Rate, Δ* (mm/sec) :**	
ZS8		**50.33**	**0.450**	
10.00	4.45	7.584	150.68	
20.00	4.75	5.415	107.58	
30.00	5.00	3.204	63.67	
40.00	5.20	2.289	45.48	
50.00	5.33	2.026	40.26	1.084
60.00	5.47	1.695	33.68	
70.00	5.58	1.498	29.77	
80.00	5.70	1.382	27.47	
90.00	5.92	1.178	23.41	

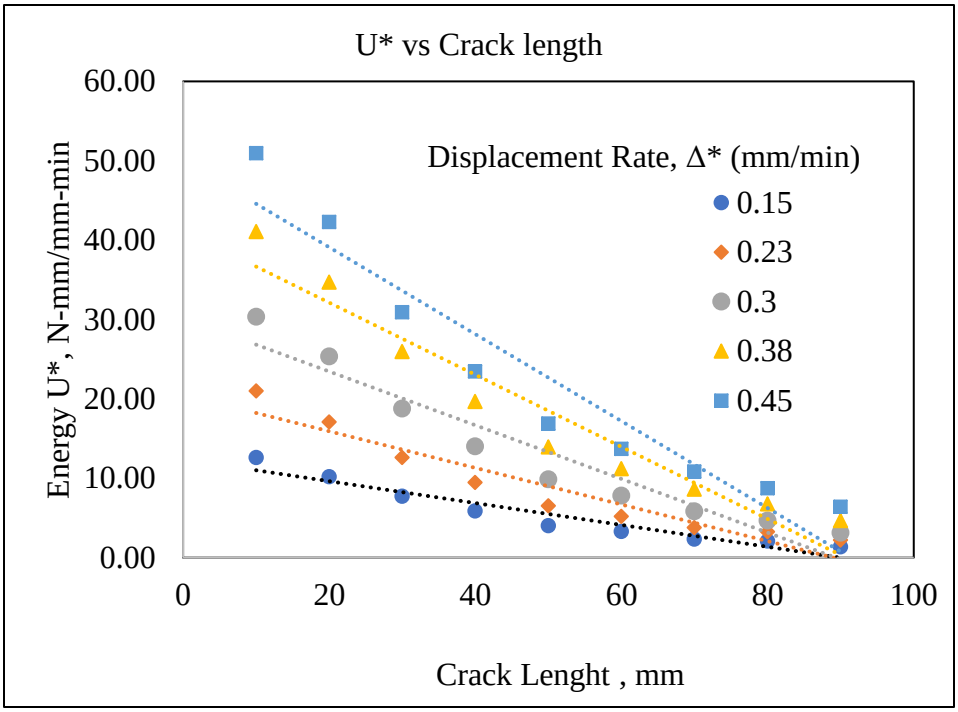

Figure 49. Energy rate vs crack length for ZT- CR samples

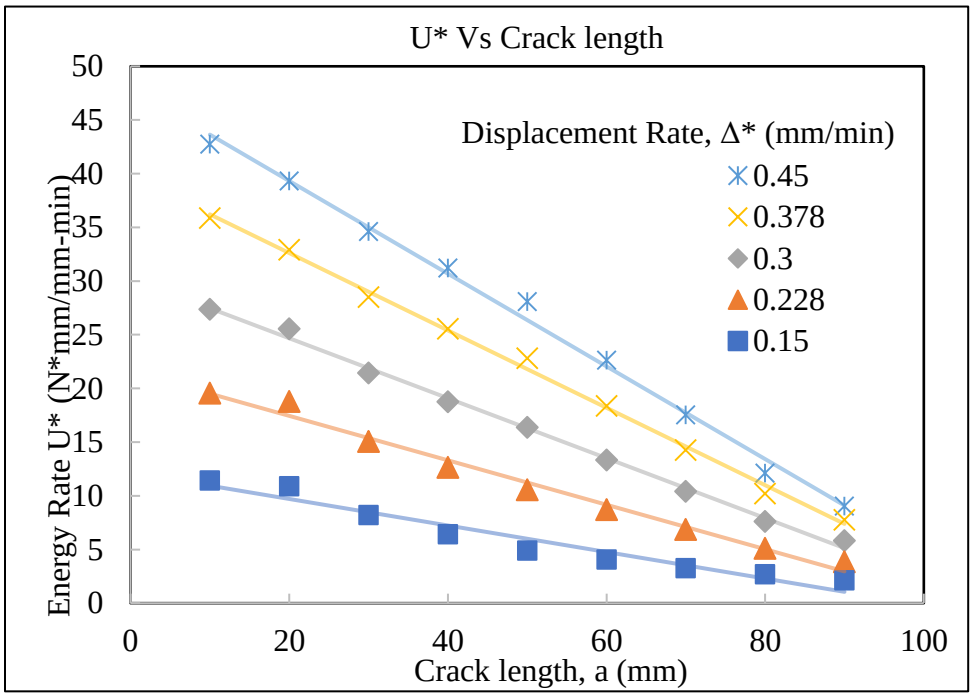

Figure 50. Energy rate vs crack length for CR samples

Figure 51. Close view of C* notch and crack propagation lines

Figure 52. C* samples after testing.

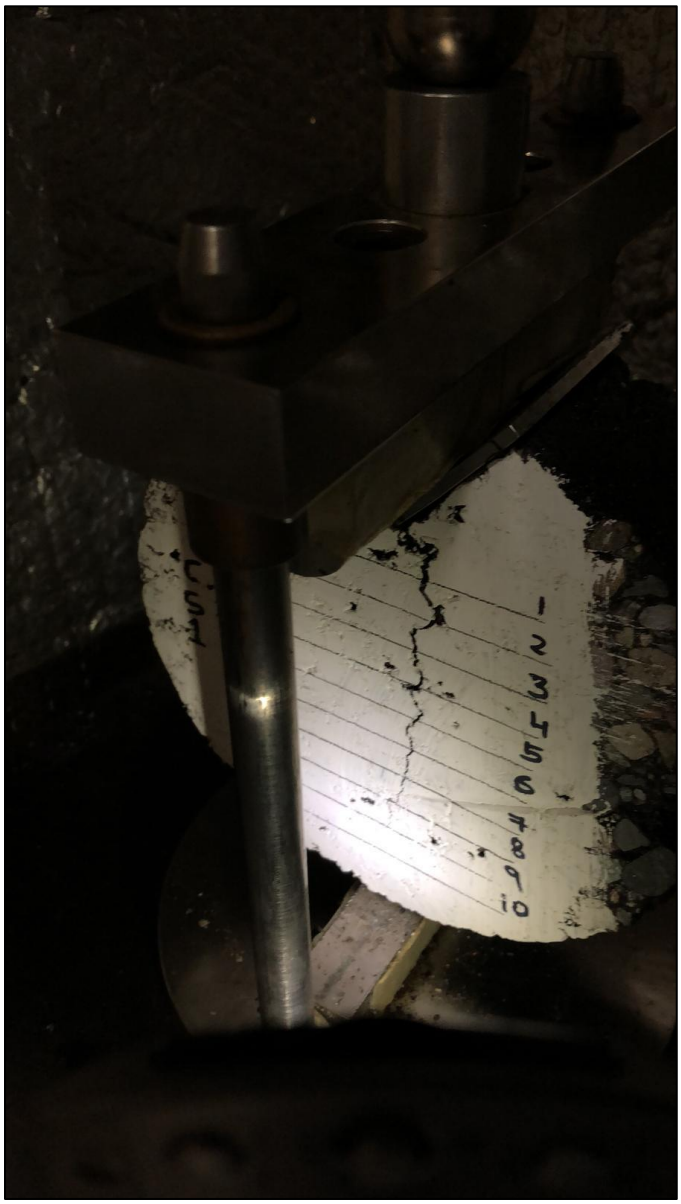

Figure 53. Crack propagation recording using a video camera with flash

APPENDIX

D. STATISTICAL HYPOTHESIS DATA

Table 28. Mean values for hypothesis testing – dynamic modulus

Temp, ºC	Frequency Hz	E* ksi		Log E* psi		Log Red Time, tr	
		CRMB	ZT	CRMB	ZT	CRMB	ZT
-10 ºC	25	3724	3463	6.57	6.54	-4.09	-4.62
	10	3532	3354	6.55	6.53	-3.69	-4.22
	5	3445	3258	6.54	6.51	-3.39	-3.92
	1	3324	2994	6.52	6.48	-2.69	-3.22
	0.5	3192	2886	6.50	6.46	-2.39	-2.92
	0.1	2786	2546	6.44	6.41	-1.69	-2.22
4.4 ºC	25	2456	2704	6.39	6.43	-4.09	-4.62
	10	2221	2517	6.35	6.40	-3.69	-4.22
	5	2059	2362	6.31	6.37	-3.39	-3.92
	1	1719	1982	6.24	6.30	-2.69	-3.22
	0.5	1596	1847	6.20	6.27	-2.39	-2.92
	0.1	1319	1526	6.12	6.18	-1.69	-2.22
21.1 ºC	25	1275	1369	6.11	6.14	-1.40	-1.40
	10	1142	1200	6.06	6.08	-1.00	-1.00
	5	1031	1082	6.01	6.03	-0.70	-0.70
	1	762	799	5.88	5.90	0.00	0.00
	0.5	667	701	5.82	5.85	0.30	0.30
	0.1	478	513	5.68	5.71	1.00	1.00
37.8 ºC	25	581	642	5.76	5.81	1.13	1.19
	10	479	526	5.68	5.72	1.53	1.59
	5	406	454	5.61	5.66	1.83	1.89
	1	255	299	5.41	5.48	2.53	2.59
	0.5	215	253	5.33	5.40	2.83	2.89
	0.1	145	171	5.16	5.23	3.53	3.59
54.4 ºC	25	225	241	5.35	5.38	1.13	1.19
	10	177	193	5.25	5.28	1.53	1.59
	5	144	158	5.16	5.20	1.83	1.89
	1	91	100	4.96	5.00	2.53	2.59
	0.5	77	83	4.88	4.92	2.83	2.89
	0.1	54	58	4.73	4.77	3.53	3.59

Table 29. Variance values for hypothesis testing – dynamic modulus

Temp, ºC	Frequency Hz	E* ksi		Log E* psi		Log Red Time, tr	
		CRMB	ZT	CRMB	ZT	CRMB	ZT
-10 ºC	25	26638	12003	0.000	0.000	0.058	0.065
	10	15502	7298	0.000	0.000	0.058	0.065
	5	18808	4013	0.000	0.000	0.058	0.065
	1	24687	6504	0.000	0.000	0.058	0.065
	0.5	21191	9298	0.000	0.000	0.058	0.065
	0.1	5584	8009	0.000	0.000	0.058	0.065
4.4 ºC	25	99899	69948	0.003	0.002	0.058	0.065
	10	43151	49712	0.002	0.001	0.058	0.065
	5	31017	39743	0.001	0.001	0.058	0.065
	1	22922	25435	0.001	0.001	0.058	0.065
	0.5	20956	24288	0.002	0.001	0.058	0.065
	0.1	13269	15388	0.001	0.001	0.058	0.065
21.1 ºC	25	6391	10932	0.001	0.001	0.000	0.000
	10	4270	7699	0.001	0.001	0.000	0.000
	5	3602	8007	0.001	0.001	0.000	0.000
	1	3172	5837	0.001	0.002	0.000	0.000
	0.5	3544	4944	0.002	0.002	0.000	0.000
	0.1	2612	5156	0.002	0.003	0.000	0.000
37.8 ºC	25	4093	4430	0.002	0.002	0.002	0.041
	10	2341	4132	0.002	0.003	0.002	0.041
	5	2164	3094	0.003	0.003	0.002	0.041
	1	736	1958	0.002	0.004	0.002	0.041
	0.5	412	1574	0.002	0.005	0.002	0.041
	0.1	117	766	0.001	0.005	0.002	0.041
54.4 ºC	25	391	719	0.002	0.003	0.002	0.041
	10	186	646	0.001	0.004	0.002	0.041
	5	79	567	0.001	0.005	0.002	0.041
	1	8	315	0.000	0.007	0.002	0.041
	0.5	0	228	0.000	0.007	0.002	0.041
	0.1	5	142	0.000	0.009	0.002	0.041

Table 30. Test statistics used for hypothesis testing - dynamic modulus

Temp, ºC	Frequency Hz	E* - ksi	Log E*	Log Red Time, s
		t'		
-10 ºC	25	2.296	2.309	2.625
	10	2.044	2.072	2.625
	5	2.145	2.186	2.625
	1	3.243	3.342	2.625
	0.5	3.034	3.094	2.625
	0.1	3.554	3.502	2.625
4.4 ºC	25	1.046	1.063	2.625
	10	1.685	1.725	2.625
	5	1.971	2.020	2.625
	1	2.072	2.105	2.625
	0.5	2.043	2.075	2.625
	0.1	2.126	2.160	2.625
21.1 ºC	25	1.243	1.266	2.185
	10	0.930	0.940	2.185
	5	0.811	0.824	2.185
	1	0.668	0.681	2.185
	0.5	0.652	0.659	2.185
	0.1	0.690	0.704	2.185
37.8 ºC	25	1.144	1.109	0.492
	10	1.022	1.006	0.492
	5	1.144	1.120	0.492
	1	1.452	1.449	0.492
	0.5	1.454	1.467	0.492
	0.1	1.539	1.593	0.492
54.4 ºC	25	0.832	0.815	0.492
	10	0.958	0.942	0.492
	5	0.963	0.951	0.492
	1	0.862	0.852	0.492
	0.5	0.748	0.733	0.492
	0.1	0.614	0.599	0.492

Table 31. Calculated degree of freedom used for hypothesis testing

Temp, ºC	Frequency Hz	E* - ksi	Log E*	Log Red Time, s
		Degrees of Freedom		
-10 ºC	25	5.00	5.21	5.97
	10	5.08	5.31	5.97
	5	3.63	3.82	5.97
	1	3.97	4.38	5.97
	0.5	4.94	5.36	5.97
	0.1	5.75	5.42	5.97
4.4 ºC	25	5.76	5.51	5.97
	10	5.96	5.98	5.97
	5	5.88	6.00	5.97
	1	5.98	5.93	5.97
	0.5	5.96	5.95	5.97
	0.1	5.96	5.95	5.97
21.1 ºC	25	5.49	5.77	5.52
	10	5.39	5.66	5.52
	5	4.99	5.31	5.52
	1	5.36	5.61	5.52
	0.5	5.79	5.95	5.52
	0.1	5.22	5.66	5.52
37.8 ºC	25	5.99	5.96	2.46
	10	5.43	5.74	2.46
	5	5.76	5.97	2.46
	1	4.64	5.26	2.46
	0.5	3.96	4.52	2.46
	0.1	3.19	3.63	2.46
54.4 ºC	25	5.36	5.56	2.46
	10	4.12	4.37	2.46
	5	3.09	3.22	2.46
	1	2.21	2.23	2.46
	0.5	2.01	2.01	2.46
	0.1	2.29	2.29	2.46

Table 32. Tabulated t-table values for α = 0.05 used for hypothesis testing

Temp, ºC	Frequency Hz	E* - ksi	Log E*	Log Red Time, s
		$t_{\alpha,v}$		
-10 ºC	25	2.78	2.57	2.57
	10	2.57	2.57	2.57
	5	3.18	3.18	2.57
	1	3.18	2.78	2.57
	0.5	2.78	2.57	2.57
	0.1	2.57	2.57	2.57
4.4 ºC	25	2.57	2.57	2.57
	10	2.57	2.57	2.57
	5	2.57	2.57	2.57
	1	2.57	2.57	2.57
	0.5	2.57	2.57	2.57
	0.1	2.57	2.57	2.57
21.1 ºC	25	2.57	2.57	2.57
	10	2.57	2.57	2.57
	5	2.78	2.57	2.57
	1	2.57	2.57	2.57
	0.5	2.57	2.57	2.57
	0.1	2.57	2.57	2.57
37.8 ºC	25	2.57	2.57	4.30
	10	2.57	2.57	4.30
	5	2.57	2.57	4.30
	1	2.78	2.57	4.30
	0.5	3.18	2.78	4.30
	0.1	3.18	3.18	4.30
54.4 ºC	25	2.57	2.57	4.30
	10	2.78	2.78	4.30
	5	3.18	3.18	4.30
	1	4.30	4.30	4.30
	0.5	4.30	4.30	4.30
	0.1	4.30	4.30	4.30

Table 33. Tabulated data for hypothesis testing – flow number

Sample	CR MIX			ZT - CR		
	Rep 1	Rep 2	Rep 2	Rep 1	Rep 2	Rep 3
Flow Number (Cycles)	1247	1479	1575	1911	1447	3095
Resilient Modulus at Failure (Mpa)	736.53	758.77	737.00	772.95	678.11	723.57
Axial Permanent Strain at Failure εp (%)	1.54	1.62	1.68	1.03	1.48	1.52
Axial Resilient Strain at Failure εr (%)	0.053	0.051	0.05	0.05	0.057	0.053
εp/εr (%)	29.11	31.73	33.56	20.58	25.91	28.60

Sample	Mean		Variance	
	CR	ZT - CR	CR	ZT - CR
Flow Number (Cycles)	1434	2151	18958	481451
Resilient Modulus at Failure (Mpa)	744	725	108	1500
Axial Permanent Strain at Failure εp (%)	1.61	1.34	0.00	0.05
Axial Resilient Strain at Failure εr (%)	0.051	0.053	1.56E-06	8.2E-06
εp/εr (%)	31.47	25.03	3.33	11.12